PHYSICAL REVIEW D **87,** 075007 (2013)

Higgs bosons in supersymmetric $U(1)'$ models with CP violation

Mariana Frank,[1,*] Levent Selbuz,[1,2,†] Levent Solmaz,[3,‡] and Ismail Turan[4,§]

[1]*Department of Physics, Concordia University, 7141 Sherbrooke Street West, Montreal, Quebec, Canada H4B 1R6*
[2]*Department of Engineering Physics, Ankara University, TR06100 Ankara, Turkey*
[3]*Department of Physics, Balıkesir University, TR10145 Balıkesir, Turkey*
[4]*Department of Physics, Middle East Technical University, TR06531 Ankara, Turkey*

(Received 18 February 2013; published 8 April 2013)

We study the Higgs sector of the $U(1)'$-extended minimal supersymmetric standard model with CP violation. This is an extension of the minimal supersymmetric standard model Higgs sector by one singlet field, introduced to generate the μ term dynamically. We are particularly interested in nonstandard decays of Higgs particles, especially of the lightest one, in the presence of CP violating phases for $\mu_{\rm eff}$ and the soft parameters. We present analytical expressions for neutral and charged Higgs boson masses at tree and one-loop levels, including contributions from top and bottom scalar quark sectors. We then study the production and decay channels of the neutral Higgs for a set of benchmark points consistent with low energy data and relic density constraints. Numerical simulations show that a Higgs boson lighter than $2m_W$ can decay in a quite distinctive manner, including invisible modes into two neutralinos ($h \to \tilde{\chi}^0\tilde{\chi}^0$) up to $\sim$50% of the time, when kinematically allowed. The branching ratio into $h \to \bar{b}b$, the dominant decay in the standard model, is reduced in some $U(1)'$ models and enhanced in others, while the branching ratios for the decays $h \to \tau^+\tau^-$, $h \to WW^*$, and $h \to ZZ^* \to 4\ell$ are always reduced with respect to their standard model expectations. This possibility has important implications for testing the $U(1)'$ model both at the LHC and later at the ILC.

DOI: 10.1103/PhysRevD.87.075007 PACS numbers: 12.60.Cn, 12.60.Jv, 14.80.Ly

I. INTRODUCTION AND MOTIVATION

Confirmation of the Higgs mechanism of the standard model (SM) of particle physics demands discovery of the elusive Higgs boson, likely seen at ATLAS [1] and CMS [2] at a mass around 126 GeV. The minimal supersymmetric extension of the SM (MSSM), which is arguably the best motivated extension of the SM, offers stabilization of the Higgs mass, and moreover agrees well with the SM predictions in certain portions of its restricted parameter space. For instance, for the upper limit of $m_h \sim 135$ GeV of the MSSM $h \to \bar{b}b$ is the dominant decay mechanism ($\sim 60\%$) in the SM and in the MSSM. On the other hand, in gauge and Higgs extended supersymmetric models, the properties of the Higgs bosons can be substantially different from that of the standard supersymmetric model predictions. For instance, the addition of one singlet field to the MSSM Higgs sector provides new tree-level contributions to the F and D terms, which stabilize the Higgs mass naturally at a larger value [3]. While many models predict a light Higgs boson around the weak scale (say $\sim$100 GeV), it will take some time to differentiate whether the boson discovered at the LHC belongs to the SM gauge symmetry, its minimal supersymmetric version (MSSM), or even to another extension such as the gauge extended versions of the MSSM.

Extensions of the gauge symmetry by an extra $U(1)$ factor (supersymmetric or not) are arguably the simplest extensions of the minimal model. The best justification for these extended models arises from assuming grand unified theories of strong and electromagnetic interactions (GUTs). In GUT symmetries, it seems difficult to break most scenarios directly to $SU(2)_L \times U(1)_Y$, as most models such as $SU(5)$, $SO(10)$, or E_6 involve an additional $U(1)$ group in the breaking. In supersymmetric $U(1)'$ models [4] [referred to as $U(1)'$ models from now on], the number of the neutral Higgs bosons is increased by an additional singlet field (S) over that of the MSSM, and the vacuum expectation value (VEV) of the singlet $\langle S \rangle$ is responsible for the generation of the μ term, which allows Higgs fields to couple to each other [5,6]; while the number of charged Higgs bosons in the $U(1)'$ extended models remains the same as in the MSSM. The interest in the Higgs sector of the $U(1)'$ models also comes from the fact that such models arise naturally from string inspired models [5,7–9], or as the dynamical solution to the μ problem in gauge-mediated supersymmetry breaking [10]. While in the MSSM and in the $U(1)'$ models lightest neutralino is the best candidate for a lightest supersymmetric particle (LSP), for the latter the LSP is less constrained.

In these models, the lightest Higgs boson could potentially behave differently from the SM or the MSSM Higgs boson due to its singlet nature. While a Higgs boson of mass $m_h \sim 126$ GeV can be predicted by the SM, or by the MSSM, or by numerous other models, the coupling of the

*mariana.frank@concordia.ca
†levent.selbuz@eng.ankara.edu.tr
‡lsolmaz@balikesir.edu.tr
§ituran@metu.edu.tr

Higgs to the known fermions or bosons is not the same in all these models. This fact can be extrapolated not only from the number of the Higgs bosons but also from their production and decay mechanisms.

Of all the Higgs bosons in a model, the properties of the lightest neutral state are the most interesting, also given its likely discovery already at the LHC. An interesting possibility is that its decay could be partially into invisible modes (a possibility hinted at by the reduced branching ratios into fermions at the LHC), or that there is another Higgs boson lighter than the one at 126 GeV, which decays completely or almost so, invisibly [11,12]. This scenario is motivated by global fits to the data at the LHC which indicate that a Higgs boson branching ratio of 64% is still unaccounted for Ref. [13].

In SM the Higgs can decay invisibly only into neutrinos, and this branching ratio is $\leq 0.1\%$ [14]. A light Higgs boson with substantial branching ratio into invisible channels can occur in a variety of models including scenarios with light neutralinos, spontaneously broken lepton number, radiatively generated neutrino masses, additional singlet scalar(s), and/or right-handed neutrinos in the extra dimensions of TeV scale gravity. Among these possibilities, invisible decay of the lightest Higgs into light neutralinos is interesting since the light neutralinos are well motivated candidates for the LSP, providing viable relic density explanations.[1] Decays into light neutralinos are possible in models with nonuniversal couplings, where LEP limits can be circumvented [17], and in models with a light dark matter candidate. For instance, a study [18] indicates that this is a possibility in E_6, where the lightest Higgs boson of the exceptional supersymmetric standard model E_6SSM can decay into the lightest neutralino pairs more than 95% of the time [19].

Additionally, the Higgs sector in extended models could provide potential sources of CP violation beyond the phase of the Cabibbo-Kobayashi-Maskawa (CKM) matrix, also important for the observed baryon asymmetry of the universe. These phases can affect the masses and couplings of the Higgs bosons to the gauge and matter fields of the model, as was shown in studies of Higgs sectors of the MSSM [20] and next-to-minimal supersymmetric models (NMSSM) [21]. The phases can also affect production and decay rate patterns, as we will show in this study. In this work, we analyze the mass spectra of all the Higgs bosons, and the production and decay rates (visible and invisible) for the lightest Higgs in the $U(1)'$ extended form of the MSSM with CP-violating phases. The masses of Higgs bosons in the $U(1)'$ with CP-violating phases model have received attention previously [22], but we include them here, for consistency with the determination of their decay properties. Thus, we revisit the Higgs sector of $U(1)'$ models and calculate the masses, and in doing this, we improve on the previous calculation by including contributions from both (s)top and (s)bottom sectors at one-loop level, and add the constraint that the lightest neutral state should have mass $\sim$125 GeV.

Motivated by the above considerations, we study anomaly-free $U(1)'$ models to probe their peculiar Higgs sector consistent with the known (astrophysical and collider) bounds, which are included in our benchmark points. We add the scalar quarks and neutralino contributions, and calculate a complete spectrum for the latter, and ensure agreement with the relic density, assuming that the lightest neutralino is the LSP. We then study the production and decay modes of the lightest neutral Higgs boson, with the purpose of unraveling the existence and consequences of invisibly decaying Higgs bosons within the $U(1)'$ model.

The outline of our study is as follows. In the following section (Sec. II) we introduce our effective $U(1)'$ model, with particular emphasis on the Higgs sector. We present tree-level (Sec. II A) and one loop mass evaluations (Sec. II B), and then an analytical calculation of the charged and neutral Higgs masses (Sec. II C). We then introduce the neutralino spectrum (Sec. II D) of the $U(1)'$ model, which contains two additional neutralinos from the MSSM. We include the constraints on the particle spectrum coming from low-energy measurements of CP violation in Sec. III, in particular from electric dipole moments (Sec. III A) and ε_K (Sec. III B). Following the exposition of the model and its constraints, we present our numerical investigations in Sec. IV, in particular for the lightest neutral Higgs boson production and decay in Sec. IV A, and comment on the second lightest neutral state in Sec. IV B. We summarize our findings and conclude in Sec. V. The full form of analytical solutions for the masses can be found in the Appendix.

II. THE $U(1)'$ MODEL WITH CP VIOLATION

We review here briefly the $U(1)'$ model, with particular emphasis to the Higgs and the neutralino sectors, as these are relevant to our study. The superpotential for the effective $U(1)'$ model is

$$W = Y_S \hat{S} \hat{H}_u \cdot \hat{H}_d + Y_t \hat{U}^c \hat{Q} \cdot \hat{H}_u + Y_b \hat{D}^c \hat{Q} \cdot \hat{H}_d, \quad (1)$$

where we assumed that all Yukawa couplings except for Y_t and Y_b are negligible. As can be seen from (1), by replacing the μ parameter with a singlet scalar (S) and a Yukawa coupling (Y_S), we resolved the μ problem of the MSSM [6]; μ is generated dynamically through the VEV of the S field (see Sec. II A) and is expected to be of the order of the weak scale.

In addition to the superpotential, the Lagrangian includes soft supersymmetry breaking terms containing additional terms with respect to the MSSM, coming from gaugino masses M_a ($a = 1, 1', 2, 3$) and trilinear couplings A_S, A_t, and A_b as given below:

[1]Note that in $U(1)'$ models the LSP can be the singlino [15,16].

$$
\begin{aligned}
-\mathcal{L}_{\text{soft}} = & \Big(\sum_a M_a \lambda_a \lambda_a + A_S Y_S S H_u \cdot H_d \\
& + A_t Y_t \tilde{U}^c \tilde{Q} \cdot H_u + A_b Y_b \tilde{D}^c \tilde{Q} \cdot H_d + \text{H.c.}\Big) \\
& + m_u^2 |H_u|^2 + m_d^2 |H_d|^2 + m_s^2 |S|^2 + M_{\tilde{Q}}^2 |\tilde{Q}|^2 \\
& + M_{\tilde{U}}^2 |\tilde{U}|^2 + M_{\tilde{D}}^2 |\tilde{D}|^2 + M_{\tilde{E}}^2 |\tilde{E}|^2 + M_{\tilde{L}}^2 |\tilde{L}|^2. \quad (2)
\end{aligned}
$$

Using renormalization group equations these soft supersymmetry (SUSY) breaking parameters are generically nonuniversal at low energies. However, in our numerical studies, we choose not to deal with the evolution of the renormalization group equations and instead assign them values which do not contradict with the current collider bounds. As we are interested in CP violation, we assume some of the soft breaking terms to be complex, selected as the trilinear terms ($A_{t,b,S}$) and the VEV of the Higgs field S, as these assignments do not conflict with present low energy data.

A. The Higgs sector at tree level

The effective $U(1)'$ model inherits two Higgs doublets H_u, H_d from the MSSM, and has an additional singlet field S, all of which can be expanded around their VEVs as

$$
\begin{aligned}
\langle H_u \rangle &= \frac{e^{i\theta_u}}{\sqrt{2}} \begin{pmatrix} \sqrt{2} H_u^+ \\ v_u + \phi_u + i\varphi_u \end{pmatrix}, \\
\langle H_d \rangle &= \frac{e^{i\theta_d}}{\sqrt{2}} \begin{pmatrix} v_d + \phi_d + i\varphi_d \\ \sqrt{2} H_d^- \end{pmatrix}, \\
\langle S \rangle &= \frac{e^{i\theta_s}}{\sqrt{2}} (v_S + \phi_S + i\varphi_S),
\end{aligned} \quad (3)
$$

in which $v^2 \equiv v_u^2 + v_d^2 = (246\ \text{GeV})^2$. The fields in the superpotential are charged under the $U(1)'$ gauge group with charges $\mathcal{Q}$, required by gauge invariance to satisfy

$$
\mathcal{Q}_{H_u} + \mathcal{Q}_{H_d} + \mathcal{Q}_S = 0, \qquad \mathcal{Q}_{Q_3} + \mathcal{Q}_{U_3} + \mathcal{Q}_{H_u} = 0,
$$
$$
\mathcal{Q}_{Q_3} + \mathcal{Q}_{D_3} + \mathcal{Q}_{H_d} = 0.
$$

The effective μ parameter is generated by the singlet VEV $\langle S \rangle$, defined as

$$
\mu_{\text{eff}} \equiv \mu e^{i\theta_s}, \quad \text{where } \mu = \frac{Y_S v_S}{\sqrt{2}}, \quad (4)
$$

so that with this convention μ is always real. For the remaining parameters we adopt the convention that the parameters are real, and explicitly attach CP-violating phases where needed. Explicitly, $\arg(A_t) = \theta_t$ and similarly θ_b refers to the argument of A_b. In order to differentiate the phase of A_S from that of S we use small and capital letters: $\arg(S) = \theta_s$, $\arg(A_S) = \theta_S$. For the Higgs fields, we assume $\theta_u = \theta_d = 0$ to avoid spontaneous CP breaking in the potential, associated with a real CKM matrix [23], which conflicts with experimental observations. However, to keep our considerations as general as possible, one can also define a new phase:

$$
\theta_\Sigma = \arg(H_u) + \arg(H_d) + \arg(S) = \theta_u + \theta_d + \theta_s. \quad (5)
$$

A detailed analysis of the Higgs sector with CP-violating phases is available in Ref. [22] and references therein, but it is sufficient to mention that we assume $\theta_s \neq 0$, which in a more general context could be replaced by $\theta_\Sigma \neq 0$. The tree-level Higgs potential of the effective $U(1)'$ model is a sum of F terms, D terms, and soft supersymmetry breaking terms:

$$
V_{\text{tree}} = V_D + V_F + V_{\text{soft}}, \quad (6)
$$

where the terms V_D, V_F, and V_{soft} are

$$
\begin{aligned}
V_D &= \frac{g^2}{8}(|H_u|^2 - |H_d|^2)^2 + \frac{g_2^2}{2}(|H_u|^2 |H_d|^2 - |H_u \cdot H_d|^2) \\
&\quad + \frac{g_{Y'}^2}{2}(\mathcal{Q}_u |H_u|^2 + \mathcal{Q}_d |H_d|^2 + \mathcal{Q}_S |S|^2)^2, \\
V_F &= |Y_S|^2 [|H_u \cdot H_d|^2 + |S|^2 (|H_u|^2 + |H_d|^2)], \\
V_{\text{soft}} &= m_{H_u}^2 |H_u|^2 + m_{H_d}^2 |H_d|^2 + m_S^2 |S|^2 \\
&\quad + (A_S Y_S S H_u \cdot H_d + \text{H.c.}),
\end{aligned} \quad (7)
$$

where the coupling constant $g^2 = g_2^2 + g_Y^2$. For the numerical analysis we take $g_Y = g_{Y'}$ [the $U(1)'$ coupling constant], which does not conflict with the unification of the gauge couplings.

From the tree-level potential, one can derive the minimization equations for the VEVs v_u, v_d, v_S and the phase $\theta_\Sigma(\theta_s)$. These relations yield conditions relating the VEVs to the physical Higgs masses.

The spectrum of physical Higgs bosons consists of three neutral scalars (h, H, H'), one CP odd pseudoscalar (A^0), and a pair of charged Higgs bosons $H^\pm$ in the CP-conserving case. In total, the spectrum differs from that of the MSSM by one extra CP-even scalar. Notice that, the composition, the mass and the couplings of the lightest Higgs boson of $U(1)'$ models can exhibit significant differences from the MSSM, and this could be an important source of distinguishing signatures in the forthcoming experiments. It is important to emphasize that these models can predict naturally larger values for m_h, the lightest neutral Higgs boson masses, which are more likely to agree with the boson mass seen at the LHC. While we can safely require $m_h \geq 90$ GeV for all numerical estimates [24], in principle, it is possible to obtain larger values such as $m_h \sim 140$ GeV within some of the E_6 based models. In our evaluations, we shall impose $m_h \sim 124$–126 GeV, in agreement with the mass of the particle observed at the LHC.

B. One-loop corrections to the Higgs potential

The tree-level potential in Eq. (6) is insufficient to make precise predictions for masses and mixings, and thus we

include loop corrections. For this we use the effective potential approach. Not all of the CP-violating parameters are free parameters, and loop corrections induce certain relationships among them. The one-loop corrected potential has the form $V = V_{\text{tree}} + \Delta V$, where V_{tree} is defined in (6), and ΔV is the one-loop Coleman-Weinberg potential [25]:

$$\Delta V = \frac{1}{64\pi^2}\left\{\Sigma_J(-1)^{2J+1}(2J+1)\mathcal{M}^4(H_u, H_d, S) \times\left[\ln\frac{\mathcal{M}^2(H_u, H_d, S)}{\Lambda^2} - \frac{3}{2}\right]\right\}, \tag{8}$$

where $\mathcal{M}$ represent the mass matrices of all the particles in the theory. While many particles and their superpartners could be added for the calculation of the loop corrections, we include here the dominant contributions coming from the top and bottom sectors ($f = t, b$) for both the quarks and scalar quarks, so that both contributions from small and large $\tan\beta$ values can be investigated safely. Specifically,

$$\Delta V = \frac{6}{64\pi^2}\sum_{f=b,t}\left\{\sum_{k=1,2}(m^2_{\tilde{f}_k})^2\left[\ln\left(\frac{m^2_{\tilde{f}_k}}{\Lambda^2}\right) - \frac{3}{2}\right] - 2(m^2_f)^2\left[\ln\left(\frac{m^2_f}{\Lambda^2}\right) - \frac{3}{2}\right]\right\}. \tag{9}$$

In this expression the masses depend explicitly on the Higgs field components: for instance, the bottom mass squared is given by $m_b^2 = Y_b^2|H_d|^2$, and the top by $m_t^2 = Y_t^2|H_u|^2$, and the scalar quark masses squared are obtained by diagonalizing the mass-squared matrix, the unitary matrix $\mathcal{S}_f$ as $\mathcal{S}_f^\dagger\tilde{M}^2\mathcal{S}_f = \text{diag}(m^2_{\tilde{f}_1}, m^2_{\tilde{f}_2})$, with $f = t, b$.

The vacuum state is obtained by requiring the vanishing of all tadpoles and positivity of the resulting Higgs boson masses. The vanishing of tadpoles for V along the CP-even directions $\phi_{H_u,H_d,S}$ and CP-odd directions $\varphi_{u,d,S}$ allows the soft masses $m^2_{H_u,H_d,S}$ to be expressed in terms of the other parameters of the potential. The tadpole terms are obtained from

$$\mathcal{T}_i = \left(\frac{\partial V}{\partial\Phi_i}\right)_0, \tag{10}$$

where $^{0000}_{0}$ means that we evaluate the derivative at the minimum of the potential, $V = V_{\text{tree}} + \Delta V$, and $\Phi_i = \phi_u$, ϕ_d, ϕ_S, φ_u, φ_d, φ_S. Since all tadpole terms must vanish, enforcement of $\mathcal{T}_{1,2,3} = 0$ is used to obtain $m_{H_u,H_d,S}$, respectively, and $\mathcal{T}_{4,5,6}$ can be used for the phase of the trilinear coupling (A_S), which is θ_S. In fact at the tree level the result is $\theta_S = 0$, but loop corrections induce this quantity to be nonzero. For instance, at the tree level, using $\mathcal{T}_1$, $\mathcal{T}_2$, and $\mathcal{T}_3$ (given explicitly in the Appendix), one can express Higgs mass squared as

$$m^2_{H_u} = \frac{A_S Y_S\cos(\theta_\Sigma + \theta_S)v_d v_S}{\sqrt{2}v_u} - \frac{\mathcal{Q}_{H_u}\Pi + Y_S^2(v_d^2 + v_S^2)}{2} + \frac{g^2(v_u^2 - v_d^2)}{8}, \tag{11}$$

$$m^2_{H_d} = \frac{A_S Y_S\cos(\theta_\Sigma + \theta_S)v_u v_S}{\sqrt{2}v_d} - \frac{\mathcal{Q}_{H_d}\Pi + Y_S^2(v_u^2 + v_S^2)}{2} + \frac{g^2(v_u^2 - v_d^2)}{8}, \tag{12}$$

$$m^2_S = \frac{A_S Y_S\cos(\theta_\Sigma + \theta_S)v_d v_u}{\sqrt{2}v_s} - \frac{\mathcal{Q}_S\Pi + Y_S^2(v_d^2 + v_u^2)}{2}, \tag{13}$$

where

$$\Pi = g^2_{Y'}(\mathcal{Q}_{H_d}v_d^2 + \mathcal{Q}_S v_S^2 + \mathcal{Q}_{H_u}v_u^2). \tag{14}$$

At tree level $\mathcal{T}_4$, $\mathcal{T}_5$, and $\mathcal{T}_6$ are zero, but at one-loop level they all induce the same nonzero result. We collected the full form of the tadpoles $\mathcal{T}_4$, $\mathcal{T}_5$, and $\mathcal{T}_6$ in the Appendix. Using the tadpoles along the CP-odd directions, the phase of the trilinear coupling of S (A_S) emerges as a radiatively induced quantity,

$$\theta_S \to -\sin^{-1}\left(\frac{3(F_b S_b A_b Y_b^2 + F_t S_t A_t Y_t^2)}{32\pi^2 A_S}\right) - \theta_\Sigma, \tag{15}$$

where we defined $S_t = \sin(\theta_t + \theta_\Sigma)$ and $S_b = \sin(\theta_b + \theta_\Sigma)$. We define cosine of the same quantities: $C_t = \cos(\theta_t + \theta_\Sigma)$ and $C_b = \cos(\theta_b + \theta_\Sigma)$. Here F_t and F_b are loop functions:

$$F_f = -2 + \ln\left(\frac{m^2_{\tilde{f}_1}m^2_{\tilde{f}_2}}{Q^4}\right) - \ln\left(\frac{m^2_{\tilde{f}_1}}{m^2_{\tilde{f}_2}}\right)\frac{\Sigma_f}{\Delta_f}, \tag{16}$$

where $f = t, b$ refers to top and bottoms and we defined Q as the SUSY breaking scale, $\Delta_f = m^2_{\tilde{f}_2} - m^2_{\tilde{f}_1}$ and $\Sigma_f = m^2_{\tilde{f}_2} + m^2_{\tilde{f}_1}$.

C. The Higgs mass calculation

We now turn to the Higgs mass calculation at one loop in the presence of CP violation in the stop and sbottom left-right mixing. The mass-squared matrix of the Higgs scalars is

$$\mathcal{M}^2_{ij} = \left(\frac{\partial^2}{\partial\Phi_i\partial\Phi_j}V\right)_0. \tag{17}$$

In the above $\Phi_i = (\phi_i, \varphi_i)$. Two linearly independent combinations of the pseudoscalar components $\varphi_{u,d,S}$ are the Goldstone bosons G_Z and $G_{Z'}$, which are used to give mass to the Z and Z' gauge bosons, leaving one physical pseudoscalar Higgs state A^0, which mixes with the neutral Higgs mass states in the presence of CP violation. In the basis of scalars $\mathcal{B} = \{\phi_u, \phi_d, \phi_S, A^0\}$, the neutral Higgs

mass-squared matrix $\mathcal{M}^2$ takes the following symmetric form:

$$\mathcal{M}^2_{H^0} = \begin{pmatrix} \mathcal{M}^2_{11} & \mathcal{M}^2_{12} & \mathcal{M}^2_{13} & \mathcal{M}^2_{14} \\ \mathcal{M}^2_{12} & \mathcal{M}^2_{22} & \mathcal{M}^2_{23} & \mathcal{M}^2_{24} \\ \mathcal{M}^2_{13} & \mathcal{M}^2_{23} & \mathcal{M}^2_{33} & \mathcal{M}^2_{34} \\ \mathcal{M}^2_{14} & \mathcal{M}^2_{24} & \mathcal{M}^2_{34} & \mathcal{M}^2_{44} \end{pmatrix}. \quad (18)$$

The mass-squared matrix can be diagonalized by a 4×4 orthonormal matrix $\mathcal{O}$. In doing this we follow the convention $\mathcal{O}\mathcal{M}^2_{H^0}\mathcal{O}^\dagger = \mathrm{diag}(m^2_{H^0_1}, m^2_{H^0_2}, m^2_{H^0_3}, m^2_{H^0_4})$, where, to avoid discontinuities in the eigenvalues, we adopt the ordering: $m_{H^0_1} < m_{H^0_2} < m_{H^0_3} < m_{H^0_4}$. The elements of $\mathcal{O}$ determine the couplings of Higgs bosons to the MSSM fermions, scalars, and gauge bosons.

The results for the entries of the neutral Higgs (mass)^2 matrix are collected in the Appendix. As an example, we show here one of the masses for the CP-conserving case. When CP is conserved all $\mathcal{M}^2_{i4}$ and $\mathcal{M}^2_{4i}$ entries should vanish, with the exception of the $\mathcal{M}^2_{44}$ term, which is actually the pseudoscalar Higgs (mass)^2 term. When CP is conserved $M^2_{A^0}$ is

$$\mathcal{M}^2_{A^0} = \mathcal{M}^2_{44} = \frac{\mu\omega^2 A_S}{v_d v_S^2 v_u} + \frac{\kappa\mu\omega^2\Delta_b^2\Delta_t^2(F_b A_b Y_b^2 + F_t A_t Y_t^2)}{v_d v_S^2 v_u}, \quad (19)$$

where $\omega^2 = v^2 v_S^2 + v_d^2 v_u^2$ and $\kappa = 3/(32\pi^2\Delta_t^2\Delta_b^2)$.

Calculation of masses of the charged Higgs bosons is very similar to the neutral ones and we obtain the following mass-squared matrix:

$$\mathcal{M}^2_{H^\pm} = \begin{pmatrix} \mathcal{M}^{2\pm}_{11} & \mathcal{M}^{2\pm}_{12} \\ \mathcal{M}^{2\pm}_{21} & \mathcal{M}^{2\pm}_{22} \end{pmatrix}, \quad (20)$$

and the eigenvalue of this matrix yields, when CP is not conserved, the expression

$$\begin{aligned} m^2_{H^\pm} = {} & \frac{\kappa\Delta_b^2\Delta_t^2}{3v^2\Sigma_b v_d v_S^2 \Sigma_t v_u}(\Sigma_t(3Y_b^2 v_S^2(F_b\Sigma_b(\mu A_b(C_b(v_d^4 + v_u^4) + 2S_b v_d^2 v_u^2) - A_b^2 v_d v_u^3 - \mu^2 v_d^3 v_u) \\ & - \Sigma_b^2 v_d v_u^3(F_b + G_b - 2) + \Delta_b^2(G_b - 2)v_d v_u^3) - \Sigma_b(v_d^4 + v_u^4)(8\pi^2 v_d v_u(4\mu^2 - g_2^2 v_S^2) - \mu\chi v_S^2) \\ & + 6Y_b^4\Sigma_b v_d^3 v_S^2 v_u^3\left(\ln\left(\frac{m_b^2}{Q^2}\right) - 1\right)) + 3\Sigma_b Y_t^2 v_S^2(F_t\Sigma_t(\mu A_t(C_t(v_d^4 + v_u^4) + 2v_d^2 S_t v_u^2) - A_t^2 v_d^3 v_u - \mu^2 v_d v_u^3) \\ & - v_d^3\Sigma_t^2 v_u(F_t + G_t - 2) + v_d^3(G_t - 2)\Delta_t^2 v_u) + 6\Sigma_b v_d^3 Y_t^4 v_S^2\Sigma_t v_u^3\left(\ln\left(\frac{m_t^2}{Q^2}\right) - 1\right)), \end{aligned} \quad (21)$$

where we defined the loop function

$$G_f = 2 + \ln\left(\frac{m^2_{\tilde{f}_1}}{m^2_{\tilde{f}_2}}\right)\frac{\Sigma_f}{\Delta_f}, \quad (22)$$

with $f = t, b$. From this it is easy to obtain the mass of the charged Higgs in the CP-conserving case. This can be achieved by taking the limits $C_t \to 1$, $C_b \to 1$ and $S_t \to 0$, $S_b \to 0$. We present explicitly the four entries of the charged Higgs mass-squared matrix in the Appendix.

D. The neutralino mass matrix in $U(1)'$

The presence of the CP-violating affects the chargino, neutralino, and scalar quark mass matrices. As we are concerned here with the (tree-level) Higgs decays into neutralinos, we show the effect on the phases on the neutralino mass matrix. Note that the chargino mass matrix is unchanged from the MSSM one, though it depends on $U(1)'$ breaking scale through the $\mu \to \mu_{\rm eff}$ parameter in the mass matrix. Similarly, the elements in the sfermion mass matrices are modified due to the presence of the Z' boson. Their explicit expressions have appeared elsewhere [26].

The neutralino sector of the $U(1)'$ is like the MSSM, but enlarged by a pair of higgsino and gaugino states, namely $\tilde{S}$ (referred to as singlino) and $\tilde{B}'$, the bare state of which we call bino-prime, while $\tilde{Z}'$ (zino-prime) is the physical mixed state. The mass matrix for the six neutralinos in the $(\tilde{B}, \tilde{W}^3, \tilde{H}_d^0, \tilde{H}_u^0, \tilde{S}, \tilde{B}')$ basis is given by a complex symmetric matrix:

$$M_{\psi^0} = \begin{pmatrix} M_1 & 0 & -M_Z c_\beta s_W & M_Z s_\beta s_W & 0 & M_K \\ 0 & M_2 & M_Z c_\beta c_W & -M_Z s_\beta c_W & 0 & 0 \\ -M_Z c_\beta s_W & M_Z c_\beta c_W & 0 & -\mu_{\rm eff} & -\mu_\lambda s_\beta & \mathcal{Q}_{H_d} M_v c_\beta \\ M_Z s_\beta s_W & -M_Z s_\beta c_W & -\mu_{\rm eff} & 0 & -\mu_\lambda c_\beta & \mathcal{Q}_{H_u} M_v s_\beta \\ 0 & 0 & -\mu_\lambda s_\beta & -\mu_\lambda c_\beta & 0 & \mathcal{Q}_S M_s \\ M_K & 0 & \mathcal{Q}_{H_d} M_v c_\beta & \mathcal{Q}_{H_u} M_v s_\beta & \mathcal{Q}_S M_s & M_1' \end{pmatrix}, \quad (23)$$

with gaugino mass parameters M_1, M_2, M_1', and M_K [27] for $\tilde{B}$, $\tilde{W}^3$, $\tilde{B}'$, and $\tilde{B}-\tilde{B}'$ mixing, respectively, $\tan\beta = v_u/v_d$, and θ_W denotes the electroweak mixing angle. After electroweak breaking there are two additional mixing parameters:

$$M_v = g_{Y'} v \quad \text{and} \quad M_s = g_{Y'} v_S. \tag{24}$$

Moreover, the doublet-doublet higgsino and doublet-singlet higgsino mass mixings are generated to be

$$\mu_{\text{eff}} = Y_S \frac{v_S}{\sqrt{2}} e^{i\theta_s}, \qquad \mu_\lambda = Y_S \frac{v}{\sqrt{2}}, \tag{25}$$

where $v = \sqrt{v_u^2 + v_d^2}$. The neutralinos mass eigenstates are Majorana spinors, and they can be obtained by diagonalization,

$$\chi_i^0 = \mathcal{N}_{ij}\psi_j, \qquad \tilde{\chi}_0 = (\chi_0, \bar{\chi}_i^0)^T. \tag{26}$$

The neutralino mass matrix is diagonalized by the same unitary matrix,

$$\mathcal{N}^\dagger M_{\chi^0} \mathcal{N} = \text{diag}(\tilde{m}_{\chi_1^0}, \ldots, \tilde{m}_{\chi_6^0}). \tag{27}$$

The additional neutralino mass eigenstates due to new higgsino and gaugino fields encode the effects of $U(1)'$ models, wherever neutralinos play a role such as in magnetic and electric dipole moments, kaon mixing, or in Higgs decays.

III. CONSTRAINTS AND IMPLICATIONS FOR THE *CP*-VIOLATING HIGGS SECTOR

A. Electric dipole moments

The experimental bounds on the electric dipole moments of the neutron $d_n < 6.3 \times 10^{-26} e$ cm and the electron $d_e < 1.8 \times 10^{-27} e$ cm [17,28], are some of the most tightly bound measurements in physics. The electric dipole moment (EDM) of a spin-$\frac{1}{2}$ particle is defined from the effective Lagrangian [29]

$$\mathcal{L}_I = -\frac{i}{2} d_f \bar{\psi} \sigma_{\mu\nu} \gamma_5 \psi F^{\mu\nu}, \tag{28}$$

and it is induced at the loop level if the theory contains a source of *CP* violation at the tree level. Unlike the SM, where the EDMs are generated through the phase of the CKM matrix at higher loop level and are thus small, in MSSM, where they are generated at one-loop level, the electric dipole moments are very important, and they provide important restrictions on the parameter space of the model. In $U(1)'$ supersymmetric models, they acquire contributions from gluinos (for neutron EDM) and chargino and neutralino (for both neutron and electron EDMs), and the contributions are generated by $\mu_{\text{eff}} = \mu e^{i\theta_s}$, with an additional contribution generated by the $\tilde{Z}'$ neutralino. The EDM was analyzed in Ref. [22] in the limit in which the sfermions are much heavier than the $\tilde{Z}'$.

The neutralino contributions to EDMs tend to be overall subdominant. To suppress the EDMs we can proceed as in the MSSM [29]: we can require that the trilinear stop coupling be mostly diagonal $A_t^{i=j} \gg A_t^{i\neq j}$ (that would suppress the sfermion contribution); we can assume cancellation between different SUSY contributions (in particular destructive interference between gluinos and charginos); or we can require that the first and second generation sfermion masses be in the TeV region. Alternatively, one can assume generically small *CP*-violating phases, a path we do not wish to follow here, not just based on naturalness, but because we wish to investigate the effects of the phases on Higgs phenomenology. In the case where $g_{Y'} = g_Y$, the case we consider here, the constraints on $U(1)'$ parameters are similar to those on the MSSM. The parameter space we choose for our benchmark points ensures that the contributions to the EDMs are sufficiently small.

B. *CP* violation in $K^0 - \bar{K}^0$ mixing

The physical phases of the Higgs singlet and in the scalar fermion, chargino and neutralino mass matrices could alter the the value of the measure of the *CP* violation in $K^0 - \bar{K}^0$ mixing, measured to be $\varepsilon_K = (2.271 \pm 0.017) \times 10^{-3}$ [17].

The contributions to the indirect *CP* violation parameter of the kaon sector, defined as

$$\varepsilon_K \simeq \frac{e^{i\pi/4}}{\sqrt{2}} \frac{\text{Im}\mathcal{M}_{12}}{\Delta m_K}, \tag{29}$$

with Δm_K the long- and short-lived kaon mass difference, and $\mathcal{M}_{12}$ the off-diagonal element of the neutral kaon mass matrix, is related to the effective Hamiltonian that governs $\Delta S = 2$ transitions as

$$\mathcal{M}_{12} = \frac{\langle K^0 | \mathcal{H}_{\text{eff}}^{\Delta S=2} | \bar{K}^0 \rangle}{2 m_K}, \quad \text{with} \quad \mathcal{H}_{\text{eff}}^{\Delta S=2} = \sum_i c_i \mathcal{O}_i. \tag{30}$$

Here c_i are the Wilson coefficients and $\mathcal{O}_i$ the corresponding four-fermion operators. In the presence of SUSY contributions, the Wilson coefficients can be decomposed as a sum,

$$c_i = c_i^W + c_i^{H^\pm} + c_i^{\tilde{\chi}^\pm} + c_i^{\tilde{g}} + c_i^{\tilde{\chi}^0},$$

where the first contribution is the SM one, the second is the charged Higgs, and the rest are supersymmetric contributions. In $U(1)'$ models, the dominant supersymmetric contributions come from the chargino mediated box diagrams, and the $\Delta S = 2$ transition is largely dominated by the $(V-A)$ operator $\mathcal{O}_1 = \bar{d}\gamma^\mu P_L s \bar{d}\gamma_\mu P_L s$, similar to the MSSM, and the chargino contribution is larger than the charged Higgs contributions. The contribution in terms of the bare chargino states is approximately [23]

TABLE I. Values of $U(1)_\eta$, $U(1)_S$, $U(1)_I$, $U(1)_N$, and $U(1)_\psi$ charges for the **27** fundamental representation of E_6 decomposition under $SO(10)$ and $SU(5)$ representations. The charge for each model is defined as $\mathcal{Q} = \cos\theta_{E_6}\mathcal{Q}_\chi + \sin\theta_{E_6}\mathcal{Q}_\psi$.

$SO(10)$ representations	$SU(5)$ representations	$2\sqrt{15}\mathcal{Q}_\eta$	$2\sqrt{15}\mathcal{Q}_S$	$2\mathcal{Q}_I$	$2\sqrt{10}\mathcal{Q}_N$	$2\sqrt{6}\mathcal{Q}_\psi$
16	**10** (u, d, u^c, e^+)	-2	$-1/2$	0	1	1
$(u, d, \nu, e^-, u^c, d^c, \nu^c, e^+)$	$\mathbf{5}^*$ (d^c, ν, e^-)	1	4	-1	2	1
	ν^c	-5	-5	1	0	1
10	**5** (H_u)	4	1	0	-2	-2
(H_u, H_d)	$\mathbf{5}^*$ (H_d)	1	$-7/2$	1	-3	-2
1 (S)	**1** (S)	-5	5/2	-1	5	4

$$\mathrm{Im}\mathcal{M}_{12} \approx \frac{2G_F^2 f_K^2 m_K M_W^4}{3\pi^2\langle m_{\tilde{q}}\rangle^8}(V_{td}^* V_{ts}) m_t^2 |m_{\tilde{W}^\pm} - \cot\beta m_{\tilde{H}^\pm}| \times \{\Delta A_t \sin\theta_s (m_{\tilde{q}}^2)_{12} I(r_{\tilde{W}^\pm}, r_{\tilde{H}^\pm}, r_{\tilde{t}_L}, r_{\tilde{t}_R})\}, \quad (31)$$

where f_K is the kaon decay constant and m_K the kaon mass; V_{ij} are the V_{CKM} elements, $\langle m_{\tilde{q}}\rangle$ is the average squark mass, taken equal to M_{SUSY}; $m_{\tilde{W}^\pm} = M_2$ is the wino mass, and $m_{\tilde{H}^\pm} = \mu$ is the higgsino mass, and $r_i = m_i^2/\langle m_{\tilde{q}}\rangle^2$. The nonuniversality in the LL soft breaking masses is parametrized by $(m_{\tilde{q}}^2)_{12}$, and the nonuniversality in the soft trilinear terms is parametrized by $\Delta A_t \equiv A_t^{13} - A_t^{23}$. Finally, I is the loop function which can be reduced to elementary functions in the limit of degenerate squark masses.

Scanning the parameter space of the model, we checked that one can find parameter sets that satisfy the minimization conditions of the Higgs potential, have an associated Higgs boson spectrum compatible with the LHC boson, and still succeed in obeying the bound for the observed value of ε_K. From Eq. (31), it appears that ε_K depends on $1/M_{\mathrm{SUSY}}^8$. To satisfy the experimental value of ε_K, values of $M_{\mathrm{SUSY}} \geq 1$ TeV would have to be assumed, or $\Delta A_t \equiv A_t^{13} - A_t^{23} \ll 1$, in agreement with our EDM considerations. Too small values of M_{SUSY} might generate a light Higgs boson spectrum already excluded by LEP and LHC, and for $M_{\mathrm{SUSY}} \sim 1$ TeV, which is consistent with our squark and slepton masses, the supersymmetric contributions to ε_K are consistent with the experimental constraints.

IV. NUMERICAL ANALYSIS

As mentioned in the Introduction, gauge extensions of the SM by one or several nonanomalous $U(1)'$ gauge groups can arise naturally from a string-inspired E_6SSM model [18,19]. In E_6SSM models the matter sector includes a **27**-representation for each family of quarks and leptons (including right-handed neutrinos), Higgs representations (doublets H_u and H_d and singlet S), and three families of extra downlike color triplets. Anomaly cancellation occurs generation by generation, and gauge coupling unification requires another pair of Higgs-like multiplets. Breaking of E_6 yields $SU(3) \times SU(2) \times U(1)_Y \times U(1)'$ as a low energy group. Anomaly-free $U(1)'$ groups are thus generated this way, directly, or as a specific linear combination. We first define the models that shall be investigated in our numerical analysis. They all emerge from breaking of higher groups [30]. For instance, the anomaly-free groups $U(1)_\psi$ [31] and $U(1)_\chi$ [32] are defined by

$$E_6 \to SO(10) \times U(1)_\psi, \qquad SO(10) \to SU(5) \times U(1)_\chi.$$

In general a $U(1)' \equiv U(1)_{E_6}$ group is defined as $U(1)_{E_6} = \cos\theta_{E_6}U(1)_\chi + \sin\theta_{E_6}U(1)_\psi$, and we distinguish among the different scenario by the values of θ_{E_6}:

(1) $\theta_\eta = \pi - \arctan\sqrt{\frac{5}{3}}$ for $U(1)_\eta$ which occurs in Calabi-Yau compactification of heterotic strings [33];
(2) $\theta_S = \arctan\sqrt{15}/9$ for the secluded $U(1)_S$, where the tension between the electroweak scale and developing a large enough Z' mass is resolved by the inclusion of additional singlets [34];
(3) $\theta_I = \arctan\sqrt{\frac{3}{5}}$ for the inert $U(1)_I$, which has a charge orthogonal to $\mathcal{Q}_\eta$ [35];
(4) $\theta_N = \arctan\sqrt{15}$ for $U(1)_N$, where ν^c has zero charge, allowing for large Majorana masses [36,37]; and
(5) $\theta_\psi = \frac{\pi}{2}$ for $U(1)_\psi$, defined above from the breaking of E_6 [31].

In Table I, we list the charges for the fundamental representations of E_6 in the $U(1)'$ models which we use for numerical investigations of Higgs boson properties.

In what follows, we investigate the consequences of each of the anomaly-free groups on the Higgs production and decay at the LHC. In Table II we list the relevant benchmark parameters for each of the choices, for both the CP-violating (CP-conserving) Higgs sectors.[2] In addition to the phase θ_s (which defines the CP-violating scenario of each model), the values of $\tan\beta$ and of μ, we give the $U(1)_Y$ and $SU(2)_L$ gaugino masses M_1 and M_2, the left- and right-hand squark soft mass parameters M_{Q_i} and M_{U_i} (all taken to be 1 TeV, including the masses in the down

[2]By CP-violating scenario, we mean the specific case where θ_s is given by the values in Table II.

TABLE II. The benchmark points (in GeV) for the *CP*-violating (*CP*-conserving) $U(1)_\eta$, $U(1)_S$, $U(1)_I$, $U(1)_N$, and $U(1)_\psi$ versions of $U(1)'$ models.

Parameters	$U(1)_\eta$	$U(1)_S$	$U(1)_I$	$U(1)_N$	$U(1)_\psi$
θ_s	42(0)	75(0)	60(0)	55(0)	33(0)
$\tan\beta$	1.8(1.7)	1.46(1.42)	1.3(2.5)	1.5(1.8)	1.75(1.75)
$\mu(\lvert\mu_{\rm eff}\rvert)$	360(360)	715(730)	465(461)	292(295)	285(290)
M_1	48(50)	56(59)	57(50)	49(50)	49(51)
M_2	125(130)	115(120)	135(120)	130(170)	140(160)
M_{Q_1}	1000(1000)	1250(850)	750(600)	2000(300)	1000(1000)
M_{Q_2}	1000(1000)	1250(850)	750(600)	2000(300)	1000(1000)
M_{Q_3}	1000(1000)	1250(850)	750(600)	2000(300)	1000(1000)
M_{U_1}	1000(1000)	1250(850)	750(600)	2000(300)	1000(1000)
M_{U_2}	1000(1000)	1250(850)	750(600)	2000(300)	1000(1000)
M_{U_3}	1000(1000)	1250(850)	750(600)	2000(300)	1000(1000)
$\lvert A_t\rvert$	1850(2000)	2200(2500)	2500(1500)	2250(2000)	2000(2000)
$\lvert A_b\rvert$	2000(2000)	2500(2500)	2500(1500)	2500(2000)	2000(2000)
$R_{Y'}$	1(1)	2.5(0.1)	0.1(6.6)	1(1)	5(5)
$R_{YY'}$	1(2.2)	0.1(0.1)	2(6.6)	6(2.7)	0.1(5)

scalar sector, not explicitly shown), the trilinear couplings in the top and bottom scalar quark sectors, A_t and A_b, and the ratios $R_{Y'} = \frac{M_1'}{M_1}$ and $R_{YY'} = \frac{M_K}{M_1}$, as defined in Ref. [26]. The constraints on the mass parameters, constraining the choice of benchmark values, are:

(1) requiring the lightest Higgs mass to be very close to 126 GeV, in agreement with the ATLAS and CMS results;
(2) requiring the next lightest neutral Higgs boson to have mass $m_{H_2^0} > 600$ GeV (as it has not been observed at LHC);
(3) requiring the lightest neutralino mass to be consistent with collider limits on Z boson decays, but also to allow for the possibility of the neutral Higgs boson to decay into a neutralino pair;
(4) choosing the lightest neutralino to be the LSP and requiring that the relic density constraint be satisfied;
(5) choosing the Z' boson mass to be consistent with present limits [17];
(6) choosing scalar masses and trilinear couplings which satisfy constraints from EDMs and *CP* violation in the kaon sector, as described in the previous section III.

As we would like to allow the Higgs boson to be kinematically allowed to decay into two neutralinos, we impose the LEP constraint on the Z boson width [38] $\Gamma(Z \to \tilde{\chi}_1^0\tilde{\chi}_1^0) < 3$ MeV. This constraint allows for a weakening of the Particle Data bound [17], especially as we do not impose the supersymmetric grand unified theory relationship $M_1 = (5/3)\tan^2\theta_W M_2$, and allow M_1 and M_2 to be free parameters, as given in Table II. Note that in particular, the bino mass is chosen to be light to allow Higgs decays into neutralinos, while value for M_2 ensures that the chargino mass will be $m_{\tilde{\chi}_1^\pm} > m_{H_1^0}/2$. The scalar fermions are heavy to satisfy bounds from the EDMs and ε_K. We choose the value of θ_s for each model to maximize the invisible decay width for the lightest Higgs boson, while satisfying the other constraints.[3]

Based on the input parameters, we calculate the spectrum of the physical masses of the extra particles in the model, which are used in our numerical evaluations. These values are given in Table III. We also included in this table the relic density of the dark matter for all scenarios. Throughout our considerations the lightest neutralino $\tilde{\chi}_1^0$ is the lightest supersymmetric particle (LSP) and thus subject to cosmological constraints. The relic calculation is straightforward using the MICROMEGAS package [40], once we include the $U(1)'$ model files from CALCHEP [41]. All the numbers are within the 1σ range of the WMAP result [42] from the Sloan Digital Sky Survey [43]:

$$\Omega_{\rm DM}h^2 = 0.111^{+0.011}_{-0.015}. \tag{32}$$

The relic density of the dark matter $\Omega_{\rm DM}h^2$ is very sensitive to the free parameter $R_{Y'}$ listed in Table II. As the lightest neutralino plays an essential role in the decay of the lightest Higgs boson, we first show the dependence of its mass, and of the relic density with the *CP*-violating parameter θ_s in Fig. 1. In all of the $U(1)'$ models under study, the lightest neutralino is mostly bino. The variations of its mass and of the relic density with the other *CP*-violating phase θ_t are negligible. Note that the mass of the LSP increases smoothly with increasing θ_s, while the relic density measurement (shown as a green band in the right-hand part of the plot) poses restrictions on the

[3]Our benchmarks are different from those of NMSSM [39], where *CP* conservation was assumed, and where the dominant decay mode of the lightest *CP*-even Higgs is into the pseudoscalar Higgs boson pairs.

TABLE III. The mass spectra (in GeV) and the relic density $\Omega_{\rm DM}$ values for the *CP*-violating (*CP*-conserving) version of the scenarios considered given in Table II for the $U(1)'$ models.

Masses	$U(1)_\eta$	$U(1)_S$	$U(1)_I$	$U(1)_N$	$U(1)_\psi$
$m_{Z'}$	1510(1510)	1507(1539)	1513(1500)	1502(1517)	1513(1540)
$m_{\tilde{\chi}_1^0}$	43(43)	55(55)	54(44)	43(42)	42(42)
$m_{\tilde{\chi}_2^0}$	108(109)	112(110)	125(107)	111(137)	114(128)
$m_{\tilde{\chi}_3^0}$	361(361)	715(730)	464(463)	292(297)	286(292)
$m_{\tilde{\chi}_4^0}$	386(388)	726(742)	485(479)	326(336)	322(331)
$m_{\tilde{\chi}_5^0}$	1487(1489)	1440(1536)	1514(1378)	1505(1498)	1396(1438)
$m_{\tilde{\chi}_6^0}$	1535(1540)	1580(1543)	1521(1711)	1556(1549)	1641(1694)
$m_{\tilde{\chi}_1^\pm}$	107(107)	111(110)	124(106)	108(134)	111(125)
$m_{\tilde{\chi}_2^\pm}$	382(384)	724(740)	481(477)	321(332)	318(326)
$m_{H_1^0}$	125.0(125.0)	125.6(125.0)	125.8(126.0)	125.6(126.0)	125.4(125.0)
$m_{H_2^0}$	743(747)	969(1027)	788(930)	642(688)	665(679)
$m_{H_3^0}$	750(754)	977(1033)	798(933)	652(695)	673(687)
$m_{H_4^0}$	1510(1510)	1508(1539)	1513(1500)	1502(1517)	1513(1540)
$m_{H^\pm}$	572(543)	717(711)	507(802)	418(504)	486(486)
$m_{\tilde{e}_L}$	1341(1341)	1837(1616)	1306(1219)	700(742)	1134(1139)
$m_{\tilde{e}_R}$	1054(1054)	1154(695)	748(598)	513(564)	1133(1137)
$m_{\tilde{\mu}_L}$	1341(1341)	1837(1616)	1306(1219)	700(742)	1134(1139)
$m_{\tilde{\mu}_R}$	1054(1054)	1154(695)	748(598)	513(564)	1133(1137)
$m_{\tilde{\tau}_1}$	1054(1054)	1154(695)	748(598)	513(564)	1133(1137)
$m_{\tilde{\tau}_2}$	1342(1341)	1837(1616)	1306(1219)	700(742)	1135(1139)
$m_{\tilde{\nu}_e}$	1340(1340)	1836(1615)	1306(1217)	699(739)	1133(1137)
$m_{\tilde{\nu}_\mu}$	1340(1340)	1836(1615)	1306(1217)	699(739)	1133(1137)
$m_{\tilde{\nu}_\tau}$	1340(1340)	1836(1615)	1306(1217)	699(739)	1133(1137)
$m_{\tilde{u}_L}$	1054(1054)	879(874)	999(998)	1106(1108)	1133(1137)
$m_{\tilde{u}_R}$	1055(1055)	882(877)	1001(1000)	1107(1109)	1134(1138)
$m_{\tilde{d}_L}$	1056(1055)	880(875)	1000(1001)	1107(1109)	1134(1139)
$m_{\tilde{d}_R}$	1340(1340)	1675(1698)	1463(1457)	1203(1207)	1133(1138)
$m_{\tilde{c}_L}$	1054(1054)	879(874)	999(998)	1106(1108)	1133(1137)
$m_{\tilde{c}_R}$	1055(1055)	882(877)	1001(1000)	1107(1109)	1134(1138)
$m_{\tilde{s}_L}$	1056(1055)	880(875)	1000(1001)	1107(1109)	1134(1139)
$m_{\tilde{s}_R}$	1340(1340)	1675(1698)	1463(1457)	1203(1207)	1133(1138)
$m_{\tilde{t}_1}$	919(911)	659(670)	788(894)	938(968)	994(1002)
$m_{\tilde{t}_2}$	1201(1207)	1085(1070)	1200(1122)	1277(1275)	1281(1283)
$m_{\tilde{b}_1}$	1056(1055)	880(875)	1000(1001)	1107(1109)	1130(1135)
$m_{\tilde{b}_2}$	1340(1340)	1675(1698)	1463(1457)	1203(1207)	1137(1141)
$\Omega_{\rm DM}$	0.114(0.120)	0.100(0.102)	0.113(0.120)	0.111(0.117)	0.117(0.101)

combined LSP mass and *CP*-violating parameter. The values of θ_s for various models listed in Table II fall into the range of the values allowed by the relic density (within the green band). We incorporate these restrictions in our analysis of Higgs mass and decay widths.

We proceed to examine the effects of the *CP*-violating phases on the masses, production cross sections, and branching ratios of the lightest Higgs boson.

A. The lightest *CP*-even neutral Higgs boson

The observation of the new boson at the LHC has fueled speculations of its nature (is it or not the SM Higgs boson), coupled with analyses of its mass and couplings, and their comparison with the experimental data. ATLAS [44] and CMS [45] have reported updates on the combined strength values for main channels, including $H^0 \to b\bar{b}$, $\gamma\gamma$, $\tau^+\tau^-$, $WW^*(\to \ell\nu\ell\nu)$ and $ZZ^*(\to 4\ell)$. While the results still have significant experimental and systematic uncertainties, these are expected to decrease with LHC operating at $\sqrt{s} =$ 14 TeV and increased luminosity. The precise determination of the Higgs couplings to different channels will establish whether the boson observed at the LHC is the SM Higgs boson. In our analysis, we wish to explore the possibility that Higgs boson decays in a non-SM fashion, in particular, that it can decay significantly invisibly. An invisible decay mode is very hard to measure directly at the colliders. However, it is not difficult to be inferred indirectly. The total decay width of a SM Higgs boson with mass of 125 GeV is approximately $\Gamma_{H^0} = 4.2$ GeV. A discrepancy between the theoretical and experimental value for the width would be an indication of additional

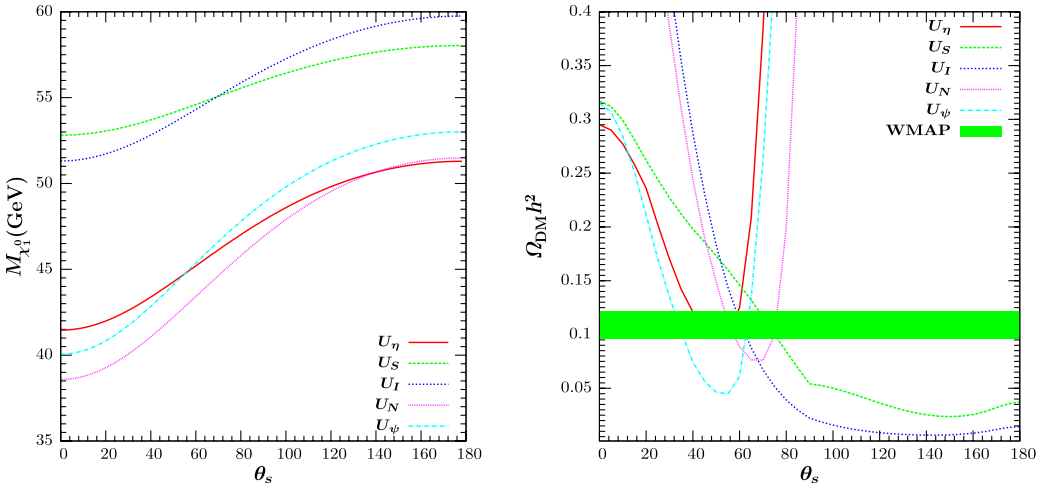

FIG. 1 (color online). Mass of the lightest neutralino and the relic density as functions of θ_s (the phase of the new singlet S) for the CP-violating versions of $U(1)_\eta$, $U(1)_S$, $U(1)_I$, $U(1)_N$, and $U(1)_\psi$ models. The green band indicates the experimentally allowed region.

decay channels beyond SM. Similarly, reduced decay branching ratios into known SM Higgs decay modes, in particular for $H^0 \to b\bar{b}$ and $H^0 \to \tau^+\tau^-$ (dominant for $m_{H^0} = 126$ GeV), could also indicate that other decays are important.

At $\tan\beta \approx 1$ the lightest Higgs mass is determined mostly by the new F and D terms in the Higgs tree-level potential, and is thus sensitive to the trilinear Yukawa coupling Y_S and the gauge coupling $g_{Y'}(= g_Y)$ in the numerical analysis. We first present our results for the dependence of the masses on the CP-violating phases $\arg(\mu_{\rm eff}) = \theta_s$ and $\arg(A_t) = \theta_t$, as well as with $\tan\beta$ in Fig. 2. One can see that the mass variations with θ_s and θ_t are significant, especially in $U(1)_S$, where large regions of the parameter space for both phases, if combined with other measurements, can be eliminated. The dependence on $\tan\beta$ from the third panel of the figure seems to indicate that only low values $\tan\beta \approx 1$–2 are allowed for all $U(1)'$ models, in agreement with the values chosen in Table II.

To analyze the decay width of the lightest Higgs boson, we first calculate total production cross section of the lightest Higgs boson (H_1^0) in various models in Table IV, for $\theta_s = 0$ (no CP violation) and for θ_s as in Table II (with CP violation). We list associated Higgs-vector boson cross sections, and the total cross section for the vector boson fusion. Though subdominant production modes for Higgs bosons, these are the dominant channels for observing an invisible decay of the Higgs boson [11]. Note that we do not include here the dominant production mechanism $gg \to H_1^0$, as this mode is plagued by large QCD corrections, and thus it is difficult to isolate the invisible decay of the Higgs boson, which in this production channel is expected to come from $gg \to H_1^0 +$ jet, and be small. As expected, the vector-boson fusion production mechanism

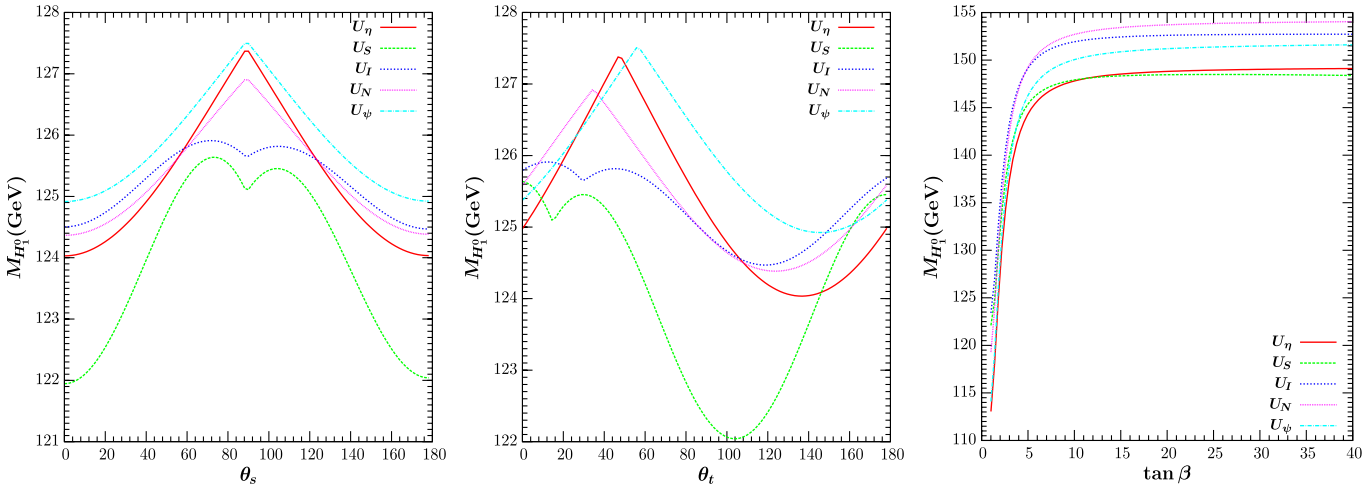

FIG. 2 (color online). Mass of the lightest neutral Higgs boson as a function of θ_s (the phase of the new singlet S), θ_t (the phase of the soft coupling A_t), and $\tan\beta$ for the CP-violating versions of $U(1)_\eta$, $U(1)_S$, $U(1)_I$, $U(1)_N$, and $U(1)_\psi$ models.

TABLE IV. Total cross sections (in fb) of associated production channel ($H_1^0 X$) and vector boson fusion production channel ($H_1^0 jj$) (in fb) for the CP-violating (CP-conserving) versions of $U(1)_\eta$, $U(1)_S$, $U(1)_I$, $U(1)_N$, and $U(1)_\psi$ models considered in the paper.

Observables	$U(1)_\eta$	$U(1)_S$	$U(1)_I$	$U(1)_N$	$U(1)_\psi$
$\sigma(pp \to H_1^0 Z)$	639(642)	631(647)	628(610)	628(624)	634(642)
$\sigma(pp \to H_1^0 W^+)$	720(725)	708(725)	705(687)	708(701)	711(720)
$\sigma(pp \to H_1^0 W^-)$	445(447)	437(448)	435(424)	437(433)	439(444)
$\sigma(pp \to H_1^0 jj(\text{VBF}))$	4983(4930)	4848(4920)	4861(4840)	4874(4850)	4873(4893)

TABLE V. Dominant branching ratios (in %) of H_1^0 decay channels for the CP-violating (CP-conserving) version of the $U(1)_\eta$, $U(1)_S$, $U(1)_I$, $U(1)_N$, and $U(1)_\psi$ scenarios considered, and in the SM.

Branching ratio	$U(1)_\eta$	$U(1)_S$	$U(1)_I$	$U(1)_N$	$U(1)_\psi$	SM
$BR(H_1^0 \to \tilde{\chi}_1^0 \tilde{\chi}_1^0)$	36.0(34.0)	8.0(2.6)	20.0(9.0)	49.0(41.0)	54.0(42)	...
$BR(H_1^0 \to b\bar{b})$	48.0(49.0)	70.0(73.0)	60.0(66.0)	38.0(44.0)	36.0(43.0)	60
$BR(H_1^0 \to \tau^- \tau^+)$	2.3(2.4)	3.5(3.6)	3.0(3.3)	1.9(2.2)	1.8(2.2)	6
$BR(H_1^0 \to WW^*)$	7.4(7.2)	10.9(11.1)	9.8(12.0)	6.1(7.5)	5.3(6.6)	21.5

dominates over the Higgs-vector boson associated production in all models. The numbers are fairly consistent across the models, and largely independent of CP-violating phases. Thus, we forgo plots of the production cross sections and expect that any differences would show up in the branching ratios of the lightest Higgs boson.

We list the dominant decay branching ratios (in %) for the lightest neutral Higgs in our model and for comparison, in the SM in Table V, again for no CP violation ($\theta_s = 0$) and with CP violation (with phases as given in Table II). The branching ratios, as well as the cross sections are largely independent of the θ_t phase. One can see that, while the production cross sections are fairly independent of the CP-violating phase θ_s, the branching ratios are not, showing significant differences between the various $U(1)'$ scenarios and the SM in the branching ratios. First, given the fact that the lightest neutralino (the LSP) has mass $m_{\tilde{\chi}_1^0} < m_{H_1^0}/2$, the Higgs boson has a considerable branching ratio into $\tilde{\chi}_1^0 \tilde{\chi}_1^0$, that is, a significant invisible width.[4] This is accompanied by a reduction in the branching ratio to other two-body decays, in particular $\tau^+\tau^-$ and WW^*. Of all the $U(1)'$ scenarios, the invisible width is the smallest in $U(1)_S$, though comparable with the decay width into $\tau^+\tau^-$ for the case of no CP violation. For the other $U(1)'$ models, the branching ratio for the invisible decay goes from a low 9% in $U(1)_I$ with no CP-violating phases, to 54% in $U(1)_\psi$ with CP violation. A general feature emerging from Table V is that the invisible width is enhanced in the presence of CP violation ($\theta_s \neq 0$) over the case with $\theta_s = 0$. This is particularly strong in the case of $U(1)_S$, where the branching ratio increases for θ_s (as in Table II) to 3 times of its CP-conserving value, and for $U(1)_I$ where it increases more than twofold. The decay into the invisible mode can reach over 50%, which is similar to the value obtained in the MSSM [46]. Note that the decay into invisible modes is sometimes at the expense of the main SM decay into $b\bar{b}$. In two of the models studied, $U(1)_S$ and $U(1)_I$, the $H_1^0 \to b\bar{b}$ branching ratio is in fact *increased* with respect to the SM value, while in $U(1)_\eta$, $U(1)_N$, and $U(1)_\psi$ it is suppressed with respect the SM expectations. But a general feature of all these models is the strong suppression of the $H_1^0 \to (W^+W^{*-} + W^{*+}W^-)$ and $H \to \tau^+\tau^*$ decay modes, expected to have a branching ratio of 21.5% and 6%, respectively, in the SM, but much smaller here. The branching ratio for the decay $H_1^0 \to \tau^+\tau^-$ is between ~2%–3.5%, while that for $H_1^0 \to WW^*$ ranges between ~5.5%–12%. In a nutshell, the Higgs decay into the invisible mode $\tilde{\chi}_1^0 \tilde{\chi}_1^0$, is at the expense of $H_1^0 \to W^+W^-$ and $\tau^+\tau^-$ in *all* models, and occasionally due to a suppression of $H_1^0 \to b\bar{b}$ in *some* models. This behavior is not unexpected, as previous studies have indicated that for light Higgs masses, the decay into neutralinos and Higgs pseudoscalar pairs (if kinematically allowed) dominate, at the expense of the SM decay modes. Increasing the lightest Higgs mass opens allowed channels, but the branching ratios are affected by the mixing with the singlet Higgs field, the pseudoscalar and the effect of the CP-violating phase. However, due to differences in decay patterns among various anomaly-free versions of the $U(1)'$ models, a more precise measurement of the Higgs boson branching ratios at the LHC will serve not only to differentiate between the SM and the $U(1)'$ model, but among the different versions of $U(1)'$'s. In Fig. 3 we plot the variation of the branching ratios of the lightest Higgs boson

[4]Note that in principle the Higgs boson can decay into sneutrinos, which can then cascade into neutralinos, contributing to the invisible width. We preclude this possibility here, as $m_{\tilde{\nu}} < m_{H^0}/2$ would require soft left-handed slepton masses of $\mathcal{O}(100)$ GeV, in conflict with the EDM constraints.

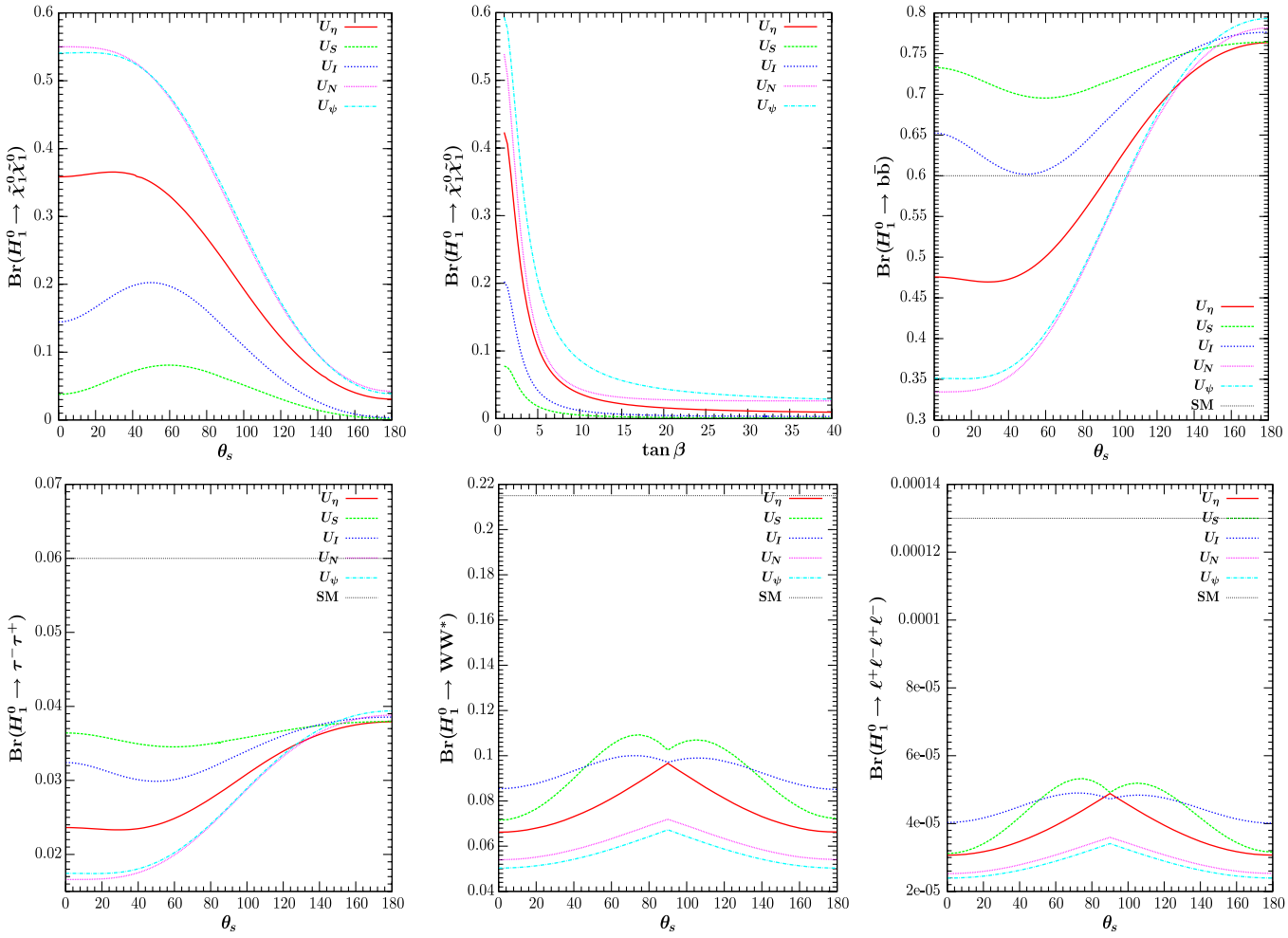

FIG. 3 (color online). $\mathrm{BR}(H_1^0 \to \chi_1^0\chi_1^0)$ as a function of θ_s and $\tan\beta$, and $\mathrm{BR}(H_1^0 \to b\bar{b})$, $\mathrm{BR}(H_1^0 \to \tau^+\tau^-)$, $\mathrm{BR}(H_1^0 \to WW^*)$, and $\mathrm{BR}(H_1^0 \to \ell^+\ell^-Z)$, as functions of θ_s for the *CP*-violating versions of $U(1)_\eta$, $U(1)_S$, $U(1)_I$, $U(1)_N$, and $U(1)_\psi$ models. When available, we also show the value of the corresponding SM quantity.

with the *CP*-violating phase θ_s. In the first two panels, we depict the dependence of the $\mathrm{BR}(H_1^0 \to \chi_1^0\chi_1^0)$ with θ_s and $\tan\beta$. As we have seen previously $\tan\beta \sim 1$–2 (as in Table II), and in that region the invisible decay width is large, and very sensitive to $\tan\beta$. We show the variation of the branching ratios of the other dominant SM and $U(1)'$ modes, as well as the that for $\mathrm{BR}(H_1^0 \to 4\ell)$, because the LHC is sensitive to this decay in the 124–126 GeV mass range, and the value is expected to become more precise. Note that we did not include any of the loop dominated decays, such as $H_1^0 \to gg$, $\gamma\gamma$, as these are sensitive to the masses and mixing parameters of the (numerous) particles in the loop, and there no new contributions to these processes with respect to MSSM. The third panel in the top row of the figure shows that, while the $\mathrm{BR}(H_1^0 \to b\bar{b})$ in SM seems to fall somewhere in the middle of predictions for $U(1)'$ models, the SM $\mathrm{BR}(H_1^0 \to \tau^+\tau^-)$ (bottom row, left side) is 6%, and outside the range of $U(1)'$ models, and so is the SM value for the $\mathrm{BR}(H_1^0 \to WW^*)$ (bottom row, middle panel). $\mathrm{BR}(H_1^0 \to 4\ell)$ (bottom row, right panel) is also beyond the upper high end of $U(1)'$ model predictions; the value expected in the SM is 0.013% while in the $U(1)'$ models, the BR's fall in the ~0.0025%–0.0055% range. The results for these decay widths might be more meaningful experimentally than the invisible Higgs width, which is difficult to measure.

B. The second lightest neutral Higgs boson

If the underlying symmetry in nature is not the SM, it is very likely that more Higgs boson states will be observed. The $U(1)'$ models all predict additional neutral and charged Higgs states. The present collider bounds indicate that the mass of the second lightest Higgs boson must be heavier than about 600 GeV. In our model, this mass shows explicit dependence on the *CP*-violating phases θ_s and θ_t. This dependence is correlated with the lightest boson mass. As the $m_H > 600$ GeV mass region will be available to LHC working at increased $\sqrt{s} = 14$ TeV, we show the mass dependence of the second lightest neutral Higgs boson in Fig. 4. The variation of this mass with either on the

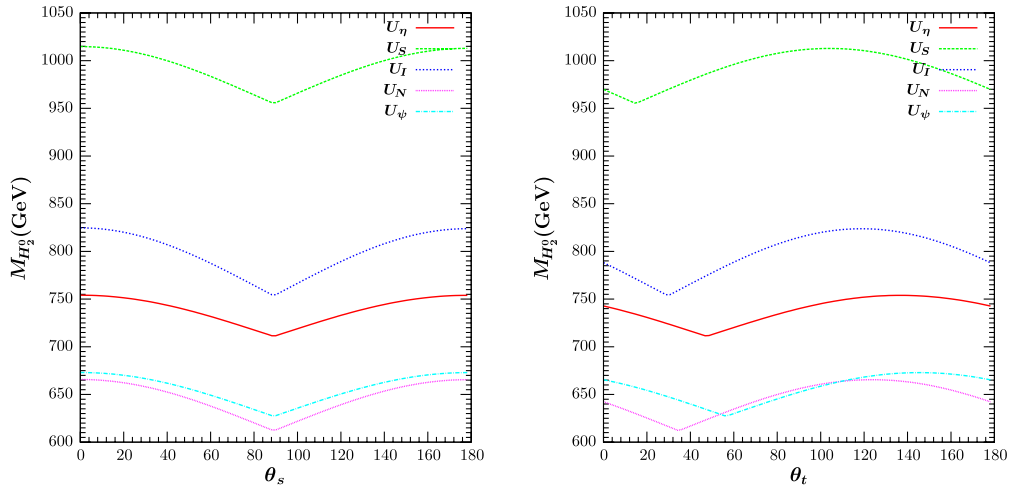

FIG. 4 (color online). $M_{H_2^0}$ as a function of θ_s (the phase of the new singlet S) and θ_t (the phase of the soft coupling A_t) for the CP-violating versions of the $U(1)_\eta$, $U(1)_S$, $U(1)_I$, $U(1)_N$, and $U(1)_\psi$ models.

CP-violating phases θ_s or θ_t is not as pronounced as for the lightest Higgs boson. Unlike in MSSM, in the majority of models under study this state appears to have a significant component of the pseudoscalar A^0. We leave the details of the decay width for later, when more experimental information could become available.

V. DISCUSSION AND CONCLUSION

The recent discovery of a Higgs-like boson at the LHC does not preclude the possibility of beyond the standard model (BSM) physics. With increased energy and luminosity, the couplings of the Higgs boson to SM particles will be measured with increased precision. In addition to the SM modes, the BSM Higgs boson can decay invisibly (to neutralinos, heavy neutrinos, or additional scalars). Our work investigates such a possibility, in a $U(1)'$-extended supersymmetric model, by analyzing the decay patterns of the lightest neutral Higgs boson. This study is motivated by the fact that the composition of the Higgs bosons is different from one in the SM or MSSM and hence, production and decay mechanisms are affected. Also significant is that $U(1)'$ models, unlike the SM, predict a light Higgs boson ($m_{H_1^0} \simeq 125$ GeV) naturally.

We chose anomaly-free versions of $U(1)'$ motivated by breaking of string-inspired E_6SSM, and study the effects for both the CP-conserving and CP-violating scenarios, and compare the lightest Higgs boson production and decay to that in the SM. Our analysis has two goals: one is to analyze effects of CP violation on Higgs masses and decays, the other is look for differences among each of the $U(1)'$ models for decay patterns, and identify characteristic signatures.

We perform a complete study of Higgs sector of the effective $U(1)'$ models, starting with calculation of masses and mixings in the Higgs sector, and including corrections from the stop and sbottom sector to one-loop level. Then we introduce benchmark scenarios for each E_6SSM motivated $U(1)'$ model, defined in terms of soft parameters, and the Higgs, Z' and sparticle spectra obtained for the benchmarks. We include a complete spectrum for the neutralinos, and include the saturation of the relic density constraint for each of the five versions of the $U(1)'$ models. Our mass spectra calculation is restricted by the inclusion of all the known constraints on the low energy spectrum, and including all the recent constraints on the lightest Higgs boson mass, and also for rare decays and cosmological constraints.

We then investigate the cross sections in channels (the vector fusion channel and the associated Higgs production with a vector boson) most propitious to look for the Higgs boson to decay invisibly. While the cross sections are not significantly affected by the CP phases (coming from the effective μ parameter and the scalar trilinear couplings), the masses and the branching ratios show significant variations. With one exception, the decay into the lightest neutralino pair is significant in all, and dominant in two of the five $U(1)'$ models under investigation. The invisible decay comes with, sometimes a suppression of the $b\bar{b}$ decay mode, from 60% to as low as 36%, except for $U(1)_S$ and $U(1)_I$, where the branching ratio is enhanced with respect to the SM, up to 73%, in the absence of CP-violating phases. All models exhibit a strong suppression of $\tau^+\tau^-$ mode (by a factor of 2–3), of WW^* (by a factor of 2–5) and of 4ℓ by the same factor. Some of these branching ratios seem to be in agreement with the present LHC data [44,45], although the measurements are not yet precise enough for a conclusive statement. The strong suppression in all $U(1)'$ models of the decay into WW^* can be traced to the mixing with the singlet, the pseudoscalar, and the CP-phase contribution, all of which are known to modify the couplings of the Higgs boson with respect to their SM values. Overall, we find that Higgs phenomenology in the $U(1)'$ model is significantly affected

by the CP phases, especially θ_s, and yields distinct signatures. The resulting signatures are unlike those of the NMSSM with CP violation, where the branching ratios of the lightest neutral Higgs boson are fairly independent of the values of CP phase θ_s [47]. Some of the signals in $U(1)'$ are typical of the anomaly-free versions of the models studied, others are characteristic for a scenario (such as the enhancement of the branching ratio into $b\bar{b}$ in $U(1)_S$ and $U(1)_I$). While other generic tests of CP violation in the supersymmetric sector exist, such as measuring chargino polarization [20], the dependence of the masses and decay patterns of the Higgs boson with the phases are a much more promising indications for CP violation in $U(1)'$. Such signatures can be probed at the LHC, and are within reach at $\sqrt{s} = 14$ TeV with luminosity $\mathcal{L} = 100$ fb^{-1}.

The decay patterns would enable to distinguish $U(1)'$ models from the SM, but also from each other. For instance, $U(1)_S$ and $U(1)_I$ show some similar decay patterns, insofar as the decay $H_1^0 \to b\bar{b}$ is dominant. Among all the models studied, $U(1)_S$ is the only one where the branching ratio of Higgs decay into neutralinos is below 10%; while in $U(1)_I$ the branching ratio into invisible modes is in the 10%–20% range. In $U(1)_\eta$, $U(1)_N$, and $U(1)_\psi$, the partial width into the invisible mode is significant, but in $U(1)_\eta$ it is still slightly below that into $b\bar{b}$. Distinguishing between $U(1)_N$ and $U(1)_\psi$ could also be based on the branching ratio into the invisible channel, which can be over 50% in $U(1)_\psi$, but under 50% in $U(1)_N$.

The characteristic signatures at the LHC would be distinctive kinematic distribution of the two quark jets in the Higgs production through vector boson fusion, compared to the Zjj and Wjj backgrounds. In the Higgs production with an associated vector boson, the ZH associated production seems more promising, as a clean signal in the dilepton + $\not{E}_T$ channel will have little background, unlike the WH model where the single lepton + $\not{E}_T$ suffers from large background effects from off-shell Drell-Yan production, as previously discussed in the literature [11]. This scenario also has consequences for other neutral Higgs states, and for the charged Higgs, the analyses of which await more data.

ACKNOWLEDGMENTS

The work of M. F. is supported in part by NSERC under Grant No. SAP105354. The research of L. S. is supported in part by The Council of Higher Education of Turkey (YOK).

APPENDIX: EXPLICIT MASS FORMULA

In this Appendix we give the complete and detailed analytical expressions used in our calculations.

1. Scalar top and scalar bottom masses

Stop and sbottom mass-squared matrices show clearly the differences between the MSSM and $U(1)'$ extended models. As can be seen from the following expressions, extra charges and gauge couplings affect LL and RR entries especially if the vacuum expectation value of the S field is sizable ($v_S \geq 1$ TeV).

The entries of the field dependent M^2 for scalar top are given by

$$\begin{aligned} M_{LL}^2 &= M_{\tilde{Q}}^2 + Y_t^2|H_u|^2 - \frac{1}{4}\left(g_2^2 - \frac{g_Y^2}{3}\right)(|H_u|^2 - |H_d|^2) \\ &\quad + g_{Y'}^2 \mathcal{Q}_Q(\mathcal{Q}_u|H_u|^2 + \mathcal{Q}_d|H_d|^2 + \mathcal{Q}_S|S|^2), \\ M_{RR}^2 &= M_{\tilde{U}}^2 + Y_t^2|H_u|^2 - \frac{g_Y^2}{3}(|H_u|^2 - |H_d|^2) \\ &\quad + g_{Y'}^2 \mathcal{Q}_U(\mathcal{Q}_u|H_u|^2 + \mathcal{Q}_d|H_d|^2 + \mathcal{Q}_S|S|^2), \\ M_{LR}^2 &= M_{RL}^{2\dagger} = Y_t(A_t^* H_u^{0*} - Y_S S H_d^0), \end{aligned} \tag{A1}$$

similarly for the scalar bottom mass squared, we have

$$\begin{aligned} M_{LL}^2 &= M_{\tilde{Q}}^2 + Y_b^2|H_d|^2 + \frac{1}{4}\left(g_2^2 + \frac{g_Y^2}{3}\right)(|H_u|^2 - |H_d|^2) \\ &\quad + g_{Y'}^2 \mathcal{Q}_Q(\mathcal{Q}_u|H_u|^2 + \mathcal{Q}_d|H_d|^2 + \mathcal{Q}_S|S|^2), \\ M_{RR}^2 &= M_{\tilde{D}}^2 + Y_b^2|H_u|^2 + \frac{g_Y^2}{6}(|H_u|^2 - |H_d|^2) \\ &\quad + g_{Y'}^2 \mathcal{Q}_D(\mathcal{Q}_u|H_u|^2 + \mathcal{Q}_d|H_d|^2 + \mathcal{Q}_S|S|^2), \\ M_{LR}^2 &= M_{RL}^{2\dagger} = Y_b(A_b^* H_d^{0*} - Y_S S H_u^0). \end{aligned} \tag{A2}$$

2. Neutral Higgs boson masses

The neutral Higgs masses are obtained by diagonalizing the 4×4 matrix in Eq. (18). The explicit values of the entries are

$$\begin{aligned} \mathcal{M}_{11}^2 = \frac{\kappa}{3\Sigma_t v_u}\Bigg[& \Sigma_t\Bigg(3\Delta_t^2\Bigg(\Delta_b^2\Bigg(2Y_t^4 v_u^3 \ln\left(\frac{m_{\tilde{t}_1}^2 m_{\tilde{t}_2}^2}{m_t^4}\right) + \mu v_d(A_b C_b F_b Y_b^2 + A_t C_t F_t Y_t^2)\Bigg) + 2\mu^2 G_b Y_b^4 v_u(A_b C_b v_d - \mu v_u)^2\Bigg) \\ & + 6A_t^2\Delta_b^2 G_t Y_t^4 v_u(\mu C_t v_d - A_t v_u)^2 + 64\pi^2\Delta_b^2\Delta_t^2\lambda_u v_u^3\Bigg) \\ & + 12A_t\Delta_b^2(G_t - 2)Y_t^4\Delta_t^2 v_u^2(\mu C_t v_d - A_t v_u) + \mu\chi\Delta_b^2 v_d\Delta_t^2\Sigma_t\Bigg], \end{aligned} \tag{A3}$$

$$\mathcal{M}^2_{12} = \frac{-\kappa}{3\Sigma_b\Sigma_t}[\Delta_t^2\Sigma_t(\Sigma_b(3\mu A_b Y_b^2(2G_b Y_b^2(A_b C_b v_d - \mu v_u)(A_b v_d - \mu C_b v_u) + C_b\Delta_b^2 F_b) - 32\pi^2\Delta_b^2 v_d v_u\lambda_{ud}) + 6\mu\Delta_b^2(G_b - 2)Y_b^4 v_d(\mu v_u - A_b C_b v_d) + \mu\chi\Delta_b^2\Sigma_b) + 6\mu\Delta_b^2\Sigma_b Y_t^4(\mu v_d - A_t C_t v_u)(A_t G_t\Sigma_t(\mu C_t v_d - A_t v_u) + (G_t - 2)\Delta_t^2 v_u) + 3\mu A_t\Delta_b^2\Sigma_b C_t F_t Y_t^2\Delta_t^2\Sigma_t], \tag{A4}$$

$$\mathcal{M}^2_{13} = \frac{\kappa}{3v_S\Sigma_t}[\Delta_t^2\Sigma_t(\Delta_b^2(3\mu F_b Y_b^2(2\mu v_u - A_b C_b v_d) + 32\pi^2 v_S^2 v_u\lambda_{us}) + 6\mu^2 G_b Y_b^4 v_u(A_b C_b v_d - \mu v_u)^2 - \mu\chi\Delta_b^2 v_d) - 3\mu A_t\Delta_b^2 C_t v_d F_t Y_t^2\Delta_t^2\Sigma_t - 6\mu\Delta_b^2 v_d Y_t^4(\mu v_d - A_t C_t v_u)(A_t G_t\Sigma_t(\mu C_t v_d - A_t v_u) + (G_t - 2)\Delta_t^2 v_u)], \tag{A5}$$

$$\mathcal{M}^2_{14} = \frac{2\kappa\mu\omega}{v_S\Sigma_t}[\Sigma_t(\mu A_b G_b Y_b^4 S_b\Delta_t^2(\mu v_u - A_b C_b v_d) + A_t^2\Delta_b^2 G_t Y_t^4 S_t(A_t v_u - \mu C_t v_d)) - A_t\Delta_b^2(G_t - 2)Y_t^4 S_t\Delta_t^2 v_u], \tag{A6}$$

$$\mathcal{M}^2_{22} = \frac{\kappa}{3\Sigma_b v_d}\Bigg[\Sigma_b\Bigg(3\Delta_t^2\Bigg(\Delta_b^2\Bigg(2Y_b^4 v_d^3\ln\Bigg(\frac{m^2_{\tilde{b}_1} m^2_{\tilde{b}_2}}{m_b^4}\Bigg) + \mu v_u(A_b C_b F_b Y_b^2 + A_t C_t F_t Y_t^2)\Bigg) + 2A_b^2 G_b Y_b^4 v_d(A_b v_d - \mu C_b v_u)^2\Bigg) + 6\mu^2\Delta_b^2 v_d G_t Y_t^4(\mu v_d - A_t C_t v_u)^2 + 64\pi^2\Delta_b^2\lambda_d v_d^3\Delta_t^2\Bigg) - 12A_b\Delta_b^2(G_b - 2)Y_b^4 v_d^2\Delta_t^2(A_b v_d - \mu C_b v_u) + \mu\chi\Delta_b^2\Sigma_b\Delta_t^2 v_u\Bigg], \tag{A7}$$

$$\mathcal{M}^2_{23} = \frac{\kappa}{3\Sigma_b v_S}[\Delta_t^2(\Sigma_b(3\mu\Delta_b^2(F_t Y_t^2(2\mu v_d - A_t C_t v_u) - A_b C_b F_b Y_b^2 v_u) - 6\mu A_b G_b Y_b^4 v_u(\mu v_u - A_b C_b v_d)(\mu C_b v_u - A_b v_d) + 32\pi^2\Delta_b^2 v_d\lambda_{ds} v_S^2) + 6\mu\Delta_b^2(G_b - 2)Y_b^4 v_d v_u(A_b C_b v_d - \mu v_u)) + 6\mu^2\Delta_b^2\Sigma_b v_d G_t Y_t^4(\mu v_d - A_t C_t v_u)^2 - \mu\chi\Delta_b^2\Sigma_b\Delta_t^2 v_u], \tag{A8}$$

$$\mathcal{M}^2_{24} = \frac{2\kappa\mu\omega}{\Sigma_b v_S}[\Sigma_b(A_b^2 G_b Y_b^4 S_b\Delta_t^2(A_b v_d - \mu C_b v_u) + \mu A_t\Delta_b^2 G_t Y_t^4 S_t(\mu v_d - A_t C_t v_u)) - A_b\Delta_b^2(G_b - 2)Y_b^4 S_b v_d\Delta_t^2], \tag{A9}$$

$$\mathcal{M}^2_{33} = \frac{\kappa}{3v_s^2}[\Delta_t^2(3\mu v_u(\Delta_b^2 v_d(A_b C_b F_b Y_b^2 + A_t C_t F_t Y_t^2) + 2\mu G_b Y_b^4 v_u(A_b C_b v_d - \mu v_u)^2] + 64\pi^2\Delta_b^2\lambda_s v_S^4) + 6\mu^2\Delta_b^2 v_d^2 G_t Y_t^4(\mu v_d - A_t C_t v_u)^2 + \mu\chi\Delta_b^2 v_d\Delta_t^2 v_u), \tag{A10}$$

$$\mathcal{M}^2_{34} = \frac{2\kappa\mu^2\omega}{v_S^2}[A_b G_b Y_b^4 S_b\Delta_t^2 v_u(\mu v_u - A_b C_b v_d) + A_t\Delta_b^2 v_d G_t Y_t^4 S_t(\mu v_d - A_t C_t v_u)], \tag{A11}$$

$$\mathcal{M}^2_{44} = \frac{\kappa\mu\omega^2}{3v_d v_S^2 v_u}[3\Delta_t^2(\Delta_b^2(A_b C_b F_b Y_b^2 + A_t C_t F_t Y_t^2) + 2\mu A_b^2 G_b Y_b^4 S_b^2 v_d v_u) + 6\mu A_t^2\Delta_b^2 v_d G_t Y_t^4 S_t^2 v_u + \chi\Delta_b^2\Delta_t^2]. \tag{A12}$$

3. *CP*-odd tadpole terms

Explicit forms of the *CP*-odd tadpole terms are

$$\begin{aligned}
\mathcal{T}_4 &= \mu A_S v_d\sin(\theta_\Sigma + \theta_S) + \frac{1}{32\pi^2}3\mu v_d(A_b F_b Y_b^2 S_b + A_t F_t Y_t^2 S_t),\\
\mathcal{T}_5 &= \mu A_S v_u\sin(\theta_\Sigma + \theta_S) + \frac{1}{32\pi^2}3\mu v_u(A_b F_b Y_b^2 S_b + A_t F_t Y_t^2 S_t),\\
\mathcal{T}_6 &= \frac{\mu A_S v_d v_u\sin(\theta_\Sigma + \theta_S)}{v_S} + \frac{1}{32\pi^2 v_S}3\mu v_d v_u(A_b F_b Y_b^2 S_b + A_t F_t Y_t^2 S_t).
\end{aligned} \tag{A13}$$

4. Charged Higgs boson masses

Finally, the charged Higgs mass is obtained by diagonalizing the matrix in Eq. (20). One of the eigenvalues will be the Goldstone boson needed to give mass to the $W^{\pm}$ boson, the other is the real charged Higgs mass. The explicit entries in (20) are

$$\begin{aligned}\mathcal{M}_{11}^{2\pm} = \frac{1}{3v^2v_S^2\Sigma_t v_u}\Big[&\kappa\Delta_b^2 v_d\Delta_t^2(\Sigma_t(\mu v_d^2 v_S^2(3A_bC_bF_bY_b^2+\chi)+3\mu A_bF_bY_b^2S_bv_S^2v_u^2+v_dv_u(8\pi^2v_d^2(g_2^2v_S^2-4\mu^2)\\&-3\mu^2F_bY_b^2v_S^2))+3Y_t^2v_S^2(A_tF_t\Sigma_t(v_u(\mu S_tv_u-A_tv_d)+\mu C_tv_d^2)-v_d\Sigma_t^2v_u(F_t+G_t-2)\\&+v_d(G_t-2)\Delta_t^2v_u)+6v_dY_t^4v_S^2\Sigma_tv_u^3\Big(\ln\Big(\frac{m_t^2}{Q^2}\Big)-1\Big)\Big)\Big],\end{aligned} \tag{A14}$$

$$\begin{aligned}\mathcal{M}_{12}^{2\pm} = \frac{1}{3v^2\Sigma_b v_S^2}\Big[&\kappa\Delta_b^2\Delta_t^2(\Sigma_b(3\mu A_tF_tY_t^2v_S^2(C_tv_u^2+v_d^2S_t)\\&+v_u(-3\mu^2v_dF_tY_t^2v_S^2+8\pi^2v_dv_u^2(g_2^2v_S^2-4\mu^2)+\mu\chi v_S^2v_u))+3Y_b^2v_S^2(A_bF_b\Sigma_b(v_u(\mu C_bv_u-A_bv_d)+\mu S_bv_d^2)\\&-\Sigma_b^2v_dv_u(F_b+G_b-2)+\Delta_b^2(G_b-2)v_dv_u)+6Y_b^4\Sigma_bv_d^3v_S^2v_u\Big(\ln\Big(\frac{m_b^2}{Q^2}\Big)-1\Big)\Big)\Big],\end{aligned} \tag{A15}$$

$$\begin{aligned}\mathcal{M}_{21}^{2\pm} = \frac{1}{3v^2v_S^2\Sigma_t}\Big[&\kappa\Delta_b^2\Delta_t^2(\Sigma_t(\mu v_d^2v_S^2(3A_bC_bF_bY_b^2+\chi)\\&+3\mu A_bF_bY_b^2S_bv_S^2v_u^2+v_dv_u(8\pi^2v_d^2(g_2^2v_S^2-4\mu^2)-3\mu^2F_bY_b^2v_S^2))+3Y_t^2v_S^2(A_tF_t\Sigma_t(v_u(\mu S_tv_u-A_tv_d)\\&+\mu C_tv_d^2)-v_d\Sigma_t^2v_u(F_t+G_t-2)+v_d(G_t-2)\Delta_t^2v_u)+6v_dY_t^4v_S^2\Sigma_tv_u^3\Big(\ln\Big(\frac{m_t^2}{Q^2}\Big)-1\Big)\Big)\Big],\end{aligned} \tag{A16}$$

$$\begin{aligned}\mathcal{M}_{22}^{2\pm} = \frac{1}{3v^2\Sigma_b v_dv_S^2}\Big[&\kappa\Delta_b^2\Delta_t^2v_u(\Sigma_b(3\mu A_tF_tY_t^2v_S^2(C_tv_u^2+v_d^2S_t)\\&+v_u(-3\mu^2v_dF_tY_t^2v_S^2+8\pi^2v_dv_u^2(g_2^2v_S^2-4\mu^2)+\mu\chi v_S^2v_u))+3Y_b^2v_S^2(A_bF_b\Sigma_b(v_u(\mu C_bv_u-A_bv_d)+\mu S_bv_d^2)\\&-\Sigma_b^2v_dv_u(F_b+G_b-2)+\Delta_b^2(G_b-2)v_dv_u)+6Y_b^4\Sigma_bv_d^3v_S^2v_u\Big(\ln\Big(\frac{m_b^2}{Q^2}\Big)-1\Big)\Big)\Big].\end{aligned} \tag{A17}$$

5. Auxiliary expressions

In the above expressions, we use the following short-hand notations:

$$\chi=\sqrt{1024\pi^4A_S^2-9(A_bF_bY_b^2S_b+A_tF_tY_t^2S_t)^2}, \tag{A18}$$

and

$$\begin{aligned}&\lambda_u=\frac{1}{2}\mathcal{Q}_u^2g_{Y'}^2+\frac{g^2}{8},\qquad \lambda_d=\frac{1}{2}\mathcal{Q}_d^2g_{Y'}^2+\frac{g^2}{8},\qquad \lambda_s=\frac{1}{2}g_{Y'}^2\mathcal{Q}_SS^2,\\&\lambda_{ud}=\mathcal{Q}_d\mathcal{Q}_ug_{Y'}^2-\frac{g^2}{4}+Y_S^2,\qquad \lambda_{ds}=\mathcal{Q}_d\mathcal{Q}_Sg_{Y'}^2+Y_S^2,\qquad \lambda_{us}=\mathcal{Q}_S\mathcal{Q}_ug_{Y'}^2+Y_S^2.\end{aligned} \tag{A19}$$

[1] G. Aad *et al.* (ATLAS Collaboration), Phys. Lett. B **716**, 1 (2012).

[2] S. Chatrchyan *et al.* (CMS Collaboration), Phys. Lett. B **716**, 30 (2012).

[3] G. G. Ross, K. Schmidt-Hoberg, and F. Staub, J. High Energy Phys. 08 (2012) 074.

[4] D. A. Demir, G. L. Kane, and T. T. Wang, Phys. Rev. D **72**, 015012 (2005).

[5] M. Cvetic, D. A. Demir, J. R. Espinosa, L. L. Everett, and P. Langacker, Phys. Rev. D **56**, 2861 (1997); **58**, 119905 (E) (1998).

[6] J. E. Kim and H. P. Nilles, Phys. Lett. B **138**, 150 (1984); D. Suematsu and Y. Yamagishi, Int. J. Mod. Phys. A **10**, 4521 (1995); M. Cvetic and P. Langacker, Mod. Phys. Lett. A **11**, 1247 (1996); V. Jain and R. Shrock, arXiv:hep-ph/9507238; Y. Nir, Phys. Lett. B **354**, 107 (1995).

[7] M. Cvetic and P. Langacker, Phys. Rev. D **54**, 3570 (1996).

[8] K. S. Babu, C. F. Kolda, and J. March-Russell, Phys. Rev. D **54**, 4635 (1996).

[9] M. Cvetic and P. Langacker, Mod. Phys. Lett. A **11**, 1247 (1996); R. Alonso, M. B. Gavela, L. Merlo, S. Rigolin, and J. Yepes, arXiv:1212.3305; arXiv:1212.3307.

[10] P. Langacker, N. Polonsky, and J. Wang, Phys. Rev. D **60**, 115005 (1999).

[11] R. M. Godbole, M. Guchait, K. Mazumdar, S. Moretti, and D. P. Roy, Phys. Lett. B **571**, 184 (2003); D. Ghosh, R. Godbole, M. Guchait, K. Mohan, and D. Sengupta, arXiv:1211.7015; O. J. P. Eboli and D. Zeppenfeld, Phys. Lett. B **495**, 147 (2000).

[12] H. Davoudiasl, T. Han, and H. E. Logan, Phys. Rev. D **71**, 115007 (2005); S. G. Frederiksen, N. Johnson, G. L. Kane, and J. Reid, Phys. Rev. D **50**, R4244 (1994); J.-J. Cao, Z. Heng, J. M. Yang, and J. Zhu, J. High Energy Phys. 06 (2012) 145.

[13] J. R. Espinosa, M. Muhlleitner, C. Grojean, and M. Trott, J. High Energy Phys. 09 (2012) 126; P. P. Giardino, K. Kannike, M. Raidal, and A. Strumia, Phys. Lett. B **718**, 469 (2012); D. Carmi, A. Falkowski, E. Kuflik, T. Volansky, and J. Zupan, J. High Energy Phys. 10 (2012) 196.

[14] A. Denner, S. Heinemeyer, I. Puljak, D. Rebuzzi, and M. Spira, Eur. Phys. J. C **71**, 1753 (2011).

[15] S. Nakamura and D. Suematsu, Phys. Rev. D **75**, 055004 (2007).

[16] D. Suematsu, Phys. Rev. D **73**, 035010 (2006).

[17] J. Beringer *et al.* (Particle Data Group), Phys. Rev. D **86**, 010001 (2012).

[18] J. P. Hall, S. F. King, R. Nevzorov, S. Pakvasa, and M. Sher, arXiv:1109.4972.

[19] J. P. Hall and S. F. King, J. High Energy Phys. 06 (2011) 006; P. Athron, S. F. King, D. J. Miller, S. Moretti, and R. Nevzorov, Proc. Sci., EPS HEP2009 (2009) 249; P. Athron, J. P. Hall, S. F. King, S. Moretti, D. J. Miller, R. Nevzorov, S. Pakvasa, and M. Sher, arXiv:1109.6373.

[20] M. Frank, T. Hahn, S. Heinemeyer, W. Hollik, H. Rzehak, and G. Weiglein, J. High Energy Phys. 02 (2007) 047; M. Frank, S. Heinemeyer, W. Hollik, and G. Weiglein, arXiv:hep-ph/0212037; S. Heinemeyer, W. Hollik, H. Rzehak, and G. Weiglein, Phys. Lett. B **652**, 300 (2007); A. Pilaftsis, Phys. Lett. B **435**, 88 (1998); A. Pilaftsis and C. E. M. Wagner, Nucl. Phys. **B553**, 3 (1999); D. A. Demir, Phys. Rev. D **60**, 055006 (1999); S. Y. Choi, M. Drees, and J. S. Lee, Phys. Lett. B **481**, 57 (2000); M. S. Carena, J. R. Ellis, A. Pilaftsis, and C. E. M. Wagner, Nucl. Phys. **B586**, 92 (2000); **B625**, 345 (2002); T. Ibrahim and P. Nath, Phys. Rev. D **63**, 035009 (2001); **66**, 015005 (2002); Y. Okada, M. Yamaguchi, and T. Yanagida, Prog. Theor. Phys. **85**, 1 (1991); J. R. Ellis, G. Ridolfi, and F. Zwirner, Phys. Lett. B **257**, 83 (1991); H. E. Haber and R. Hempfling, Phys. Rev. Lett. **66**, 1815 (1991); S. W. Ham, S. K. Oh, E. J. Yoo, C. M. Kim, and D. Son, Phys. Rev. D **68**, 055003 (2003).

[21] T. Graf, R. Grober, M. Muhlleitner, H. Rzehak, and K. Walz, J. High Energy Phys. 10 (2012) 122; K. Cheung, T.-J. Hou, J. S. Lee, and E. Senaha, Phys. Rev. D **82**, 075007 (2010); K. Funakubo and S. Tao, Prog. Theor. Phys. **113**, 821 (2005); S. W. Ham, S. K. Oh, and D. Son, Phys. Rev. D **65**, 075004 (2002); S. W. Ham, Y. S. Jeong, and S. K. Oh, arXiv:hep-ph/0308264.

[22] D. A. Demir and L. L. Everett, Phys. Rev. D **69**, 015008 (2004).

[23] G. C. Branco, F. Kruger, J. C. Romao, and A. M. Teixeira, J. High Energy Phys. 07 (2001) 027; C. Hugonie, J. C. Romao, and A. M. Teixeira, J. High Energy Phys. 06 (2003) 020.

[24] D. A. Demir, L. Solmaz, and S. Solmaz, Phys. Rev. D **73**, 016001 (2006).

[25] S. R. Coleman and E. J. Weinberg, Phys. Rev. D **7**, 1888 (1973).

[26] D. A. Demir, M. Frank, L. Selbuz, and I. Turan, Phys. Rev. D **83**, 095001 (2011).

[27] S. Y. Choi, H. E. Haber, J. Kalinowski, and P. M. Zerwas, Nucl. Phys. **B778**, 85 (2007).

[28] B. C. Regan, E. D. Commins, C. J. Schmidt, and D. DeMille, Phys. Rev. Lett. **88**, 071805 (2002); C. A. Baker *et al.*, Phys. Rev. Lett. **97**, 131801 (2006).

[29] T. Ibrahim and P. Nath, Phys. Rev. D **57**, 478 (1998); **58**, 019901(E) (1998); **60**, 079903(E) (1999); **60**, 119901(E) (1999); S. Abel, S. Khalil, and O. Lebedev, Nucl. Phys. **606B**, 151 (2001).

[30] P. Langacker, Rev. Mod. Phys. **81**, 1199 (2009).

[31] P. Langacker and J. Wang, Phys. Rev. D **58**, 115010 (1998); R. N. Mohapatra, *Unification and Supersymmetry: The Frontiers of Quark-Lepton Physics* (Springer, Berlin, 2003).

[32] J. L. Hewett and T. G. Rizzo, Phys. Rep. **183**, 193 (1989).

[33] E. Witten, Nucl. Phys. **B258**, 75 (1985).

[34] J. Erler, P. Langacker, and T.-j. Li, Phys. Rev. D **66**, 015002 (2002).

[35] R. W. Robinett and J. L. Rosner, Phys. Rev. D **26**, 2396 (1982).

[36] V. Barger, P. Langacker, and H.-S. Lee, Phys. Rev. D **67**, 075009 (2003); J. Kang and P. Langacker, Phys. Rev. D **71**, 035014 (2005); E. Ma, Phys. Lett. B **380**, 286 (1996).

[37] S. F. King, S. Moretti, and R. Nevzorov, Phys. Rev. D **73**, 035009 (2006).

[38] S. Schael *et al.* [ALEPH, DELPHI, L3, OPAL, SLD, LEP Electroweak Working Group, SLD Electroweak Group, SLD Heavy Flavour Group Collaborations], Phys. Rep. **427**, 257 (2006).

[39] A. Djouadi, M. Drees, U. Ellwanger, R. Godbole, C. Hugonie, S. F. King, S. Lehti, S. Moretti *et al.*, J. High Energy Phys. 07 (2008) 002.

[40] G. Belanger, F. Boudjema, A. Pukhov, and A. Semenov, Comput. Phys. Commun. **180**, 747 (2009); G. Belanger, F. Boudjema, P. Brun, A. Pukhov, S. Rosier-Lees, P. Salati, and A. Semenov, Comput. Phys. Commun. **182**, 842 (2011).

[41] See http://theory.sinp.msu.ru/~pukhov/calchep.html; A. Pukhov, arXiv:hep-ph/0412191.
[42] E. Komatsu *et al.* (WMAP Collaboration), Astrophys. J. Suppl. Ser. **192**, 18 (2011).
[43] D. N. Spergel *et al.* (WMAP Collaboration), Astrophys. J. Suppl. Ser. **170**, 377 (2007).
[44] G. Aad *et al.* (ATLAS Collaboration), Report No. ATLAS-CONF-2012-168, 169, 170.
[45] S. Chatrchyan *et al.* (CMS Collaboration), Report No. CMS-PAS-HIG-12-045.
[46] D. Albornoz Vasquez, G. Belanger, R. M. Godbole, and A. Pukhov, Phys. Rev. D **85**, 115013 (2012).
[47] S. W. Ham, S. H. Kim, S. K. Oh, and D. Son, Phys. Rev. D **76**, 115013 (2007); S. W. Ham, J. O. Im, and S. K. Oh, Eur. Phys. J. C **58**, 579 (2008).